

# Spectral and algebraic instabilities in thin Keplerian discs under poloidal and toroidal magnetic fields

Yuri M. Shtemler<sup>1\*</sup>, Michael Mond<sup>1</sup>, and Edward Liverts<sup>1</sup>

<sup>1</sup>*Department of Mechanical Engineering, Ben-Gurion University of the Negev, P.O. Box 653, Beer-Sheva 84105, Israel*

Accepted —. Received —; in original form —

## ABSTRACT

Linear instability of two equilibrium configurations with either poloidal (I) or toroidal (II) dominant magnetic field components are studied in thin vertically-isothermal Keplerian discs. Solutions of the stability problem are found explicitly by asymptotic expansions in the small aspect ratio of the disc. In both equilibrium configurations the perturbations are decoupled into in-plane and vertical modes. For equilibria of type I those two modes are the Alfvén-Coriolis and sound waves, while for equilibria of type II they are the inertia-Coriolis and magnetosonic waves. Exact expressions for the growth rates as well as the number of unstable modes for type I equilibria are derived. Those are the discrete counterpart of the continuous infinite homogeneous cylinder magnetorotational (MRI) spectrum. The axisymmetric MRI is completely suppressed by large toroidal magnetic fields and leaves the system exclusively to the non-modal algebraic growth mechanism which occurs due to the rotation shear. This generates the inertia-Coriolis driven magnetosonic modes and leads to their non-resonant or resonant coupling that induces, respectively, the linear or quadratic in time growth of perturbations.

**Key words:** accretion, accretion discs - MHD-instabilities

## 1 INTRODUCTION

The stability properties of Keplerian disks have been a focus of intensive investigation of theoretical astrophysicists over the last decades, pertaining to the problem of angular momentum transfer in accretion disks. Traditionally, two routes have been taken by researchers in order to elucidate various aspects of that topic. Thus, the results of the analytical study of magneto-rotational instability (MRI) in an infinitely long cylinder [Velichov (1959); Chandrasechar (1960)] have been adopted for the thin disks in order to derive criteria for the spectral stability under various conditions [Balbus & Hawley (1991)]. On the second route, numerical calculations have been performed, usually by employing the shearing-box model, in order to study the nonlinear evolution of small perturbations, and their subsequent development into full sustainable turbulence [Bodo et al. (2008); Regev & Umrhan (2008)]. The main thrust of both routes has been to establish the MRI as the main generator of sustainable turbulence. Notwithstanding accumulating analytical as well as numerical results, the notion of the MRI as a driver of turbulence and angular momentum transport has recently been shown to suffer from non-trivial difficulties in the sheer use of the shearing box in the simulations [Bodo et al. (2008); Regev & Umrhan (2008)] as well as in doubts regarding the numerical convergence and resolution [Lesur & Longaretti (2007); Fromang & Papaloizou (2007); Fromang et al. (2007); Pessah et al. (2007)]. In addition, it has recently been shown that if the thin disk geometry is taken into account both the growth rates as well as the number of unstable MRI modes are greatly reduced and are decreasing functions of the disk thickness [Coppi & Keyes (2003); Liverts & Mond (2009)]. In parallel, an alternative route that has recently emerged within which the dynamical response of the thin disks is investigated asymptotically in the small thickness-to-radius ratio has been shown to lead to fruitful and physically sound results. In particular, applying such strategy it has been shown that algebraic non-modal instabilities are the primary source of pure hydrodynamical activity [Umrhan et al. (2006); Rebusco et al. (2009)];

\* E-mail: shtemler@bgu.ac.il; mond@bgu.ac.il; eliverts@bgu.ac.il

Shtemler et al. (2010)]. Furthermore, the mechanism for such non-exponential growth has been identified as the resonant as well as non-resonant interaction between inertia-Coriolis modes and sound waves [Shtemler et al. (2010)]. Interestingly enough, such an investigation has never been carried out for magnetized disks that are described by the magnetohydrodynamic (MHD) model. It is thus one of the main goals of the current work to carry out a comprehensive study of the MHD response of thin Keplerian disks taking into account their true thin-disk geometry.

In that connection note that although the magnetic field configuration in real discs is largely unknown, in the initial stage of the disc rotation the poloidal field is commonly accepted as the dominant component. However, observations and numerical simulations indicate that toroidal magnetic field may be of the same order of magnitude, or even dominate the poloidal magnetic field [see e.g. Terquem & Papaloizou (1996); Papaloizou & Terquem (1997); Hawley & Krolik (2002); Proga (2003)]. In particular, the unstable modes give rise to MRI [Balbus & Hawley (1991)] which amplifies considerably the toroidal component of the magnetic field to the point that it may dominate the original axial field [Pessah & Psaltis (2005); Begelman & Pringle (2007)]. It is of great importance therefore to investigate how the magnetic field topology influences the stability properties of the disc. The way to do that is to follow the linear problem in terms of a toroidal dominated magnetic field instead of poloidal one leading to MRI. Thus, one more goal of the present work is investigation of two types of magnetic field equilibrium configurations with either poloidal or toroidal dominated magnetic field component and their relations with spectral and non-modal mechanisms of instability in thin discs.

The paper is organized as follows. The dimensionless governing equations and their approximation to leading order in small aspect ratio of the steady-state disc are presented in the next Section. Two magnetic field configurations with dominated axial (I) and toroidal (II) equilibrium magnetic fields are also described in that Section. Sections 3 and 4 describe the principal hydro-magnetic modes which can propagate in thin Keplerian discs for I and II types of equilibria, respectively. Summary and discussion are presented in Section 5.

## 2 THE PHYSICAL MODEL FOR THIN KEPLERIAN DISCS

The stability of radially as well as axially stratified rotating plasma in thin vertically isothermal discs threaded by a magnetic field is considered. Viscosity, electrical resistivity, and radiation effects are ignored.

### 2.1 Governing equations

As a first step, all physical variables are transformed to non-dimensional quantities by using the following characteristic values [Shtemler et al. (2009); Shtemler et al. (2010)]:

$$t_* = \frac{1}{\Omega_*}, \quad V_* = \frac{r_*}{t_*}, \quad L_* = V_* t_*, \quad m_* = m_i, \quad n_* = n_i,$$

$$\Phi_* = V_*^2, \quad c_{S*} = \sqrt{T_*/m_*}, \quad P_* = m_* n_* c_{S*}^2, \quad j_* = \frac{c}{4\pi} \frac{B_*}{r_*}, \quad E_* = \frac{V_* B_*}{c}. \quad (1)$$

Here  $\Omega_* = (GM_c/r_*^3)^{1/2}$  is the Keplerian angular velocity of the fluid at the characteristic radius  $r_*$  that belongs to the Keplerian portion of the disc;  $G$  is the gravitational constant;  $M_c$  is the total mass of the central object;  $c$  is the speed of light;  $\Phi_*$  is the characteristic value of the gravitational potential; the characteristic mass and number density equal to the ion mass and number density,  $m_* = m_i$  and  $n_* = n_i$ . The characteristic values of the electric current density and electric field,  $j_*$  and  $E_*$  have been chosen consistently with Maxwell's equations;  $c_{S*}$  is the characteristic sound velocity;  $T_* = T(r_*)$  is the characteristic temperature; the characteristic magnetic field is specified below depending on the magnetic field configuration:  $B_* = B_z(r_*)$  if the axial equilibrium magnetic field dominates or of the order toroidal one, and  $B_* = B_\theta(r_*)$  otherwise; the dimensional equilibrium temperature and the two components of the equilibrium magnetic field,  $T(r)$  and  $B_z(r)$ ,  $B_\theta(r)$ , respectively, are free functions.

The resulting dimensionless dynamical equations for vertically isothermal discs are:

$$\frac{D\mathbf{V}}{Dt} = -\frac{1}{M_S^2} \frac{\nabla P}{n} - \nabla\Phi + \frac{1}{\beta M_S^2} \frac{\mathbf{j} \times \mathbf{B}}{n}, \quad (2)$$

$$\frac{\partial n}{\partial t} + \nabla \cdot (n\mathbf{V}) = 0, \quad (3)$$

$$\frac{\partial \mathbf{B}}{\partial t} + \nabla \times \mathbf{E} = 0, \quad \nabla \cdot \mathbf{B} = 0, \quad (4)$$

$$\mathbf{E} = -\mathbf{V} \times \mathbf{B}, \quad (5)$$

$$P = nT. \quad (6)$$

Here  $\nabla P = \bar{c}_S^2 \nabla n$  for vertically isothermal discs, and the dimensionless equilibrium sound speed is given by  $\bar{c}_S^2 = \partial P / \partial n \equiv T(r)$ . Standard cylindrical coordinates  $\{r, \theta, z\}$  are adopted throughout the paper with the associated unit vectors  $\{\mathbf{i}_r, \mathbf{i}_\theta, \mathbf{i}_z\}$ ;  $\mathbf{V}$  is the plasma velocity;  $t$  is time;  $D/Dt = \partial/\partial t + (\mathbf{V} \cdot \nabla)$  is the material derivative;  $\Phi(r, z) = -(r^2 + z^2)^{-1/2}$  is the gravitational potential due to the central object;  $\mathbf{B}$  is the magnetic field,  $\mathbf{j} = \nabla \times \mathbf{B}$  is the current density;  $\mathbf{E}$  is the electric field;  $P = P_e + P_i$  is the total plasma pressure;  $P_l = n_l T_l$  are the partial species pressures ( $l = e, i$ );  $T = T_e = T_i$  is the plasma temperature; subscripts  $e$  and  $i$  denote electrons and ions, respectively. Note that a preferred direction is tacitly defined here, namely, the positive direction of the  $z$  axis is chosen according to positive Keplerian rotation. The dimensionless coefficients  $M_S$  and  $\beta$  are the Mach number and the characteristic plasma beta, respectively:

$$M_S = \frac{V_*}{c_{S*}}, \quad \beta = \frac{P_*}{B_*^2}. \quad (7)$$

Zero conditions at infinity for the in-plane magnetic field are adopted, namely:

$$B_r = 0, \quad B_\theta = 0 \quad \text{for } z = \pm\infty. \quad (8)$$

The boundary condition for the axial velocity will be specified below as the least possible divergence at infinity. As will be seen later on, despite such unbounded growth the axial mass flux tends to zero far away from the mid-plane due to the fast vanishing of number density at  $\zeta = \pm\infty$ . To simplify the further treatment of Maxwell's equations, both the hydro-magnetic basic configuration and perturbations are assumed to be axisymmetric.

A common property of thin Keplerian discs is their highly compressible motion with large Mach numbers [Frank et al. (2002)]. Furthermore, the characteristic effective semi-thickness of the equilibrium disc  $H_* = H(r_*)$  ( $H = H(r)$  is the local semi-thickness) is defined so that the disc aspect ratio  $\epsilon$  equals the inverse Mach number:

$$\frac{1}{M_S} = \epsilon = \frac{H_*}{r_*} \ll 1. \quad (9)$$

Thus, the thin disc approximation means

$$\frac{1}{M_S} = \sqrt{\frac{r_* T_*}{GM_c}} = \epsilon \ll 1, \quad (10)$$

where

$$M_S = \frac{V_*}{c_{S*}}, \quad V_* = r_* \Omega_*, \quad \Omega_* = \sqrt{\frac{GM_c}{r_*^3}}, \quad c_{S*} = \sqrt{T_*}, \quad H_* = \frac{c_{S*}}{\Omega_*}.$$

The smallness of  $\epsilon$  means that dimensionless axial coordinate is also small, i.e.  $z/r_* \sim \epsilon$  ( $|z| \lesssim H_*$ ), and consequently the following rescaled quantities may be introduced in order to further apply the asymptotic expansions in  $\epsilon$  [similar to Shtemler et al. (2009); Shtemler et al. (2010)]:

$$\zeta = \frac{z}{\epsilon} \sim \epsilon^0, \quad \bar{H}(r) = \frac{H(r)}{\epsilon} \sim \epsilon^0, \quad (11)$$

where  $\bar{H}(r) = \bar{c}_S / \bar{\Omega}(r)$  is the scaled semi-thickness of the disc.

## 2.2 Equilibrium configurations

We start by deriving the steady state solution. It is first noted that the asymptotic expansion for the time-independent gravitational potential is given by:

$$\bar{\Phi}(r, \zeta) = \bar{\Psi}(r) + \epsilon^2 \bar{\psi}(r, \zeta), \quad \bar{\Psi}(r) = -\frac{1}{r}, \quad \bar{\psi}(r, \zeta) = \frac{1}{2} \zeta^2 \bar{\Omega}^2(r) + O(\epsilon^2), \quad r > 1 \gg \epsilon. \quad (12)$$

Substituting (12) into Eqs. (2)-(6) and setting the partial derivatives with respect to time to zero yield to leading order in  $\epsilon$

$$\frac{\bar{V}_\theta^2}{r} = \frac{d\bar{\Psi}(r)}{dr}, \quad \frac{\bar{c}_S^2(r)}{\bar{n}} \frac{\partial \bar{n}}{\partial \zeta} = -\frac{\partial \bar{\psi}(r, \zeta)}{\partial \zeta}. \quad (13)$$

Thus, the velocity as well as the number density are as follows:

$$V_r = o(\epsilon), \quad V_\theta(r) = \epsilon^0 \bar{V}_\theta(r) + O(\epsilon^2), \quad V_z = o(\epsilon^2), \quad n = \epsilon^0 \bar{n}(r, \zeta) \equiv \epsilon^0 \bar{N}(r) \bar{\nu}(\eta), \quad (14)$$

where  $o(\epsilon) \ll \epsilon$ ,  $O(\epsilon) \sim \epsilon$ , and

$$\bar{V}_\theta(r) = r \bar{\Omega}(r), \quad \bar{\Omega}(r) = r^{-3/2}, \quad \bar{\nu}(\eta) = \exp(-\eta^2/2), \quad \eta = \zeta / \bar{H}(r). \quad (15)$$

Two quite different equilibrium magnetic configurations will be considered below, namely one with comparable magnitudes of the axial and toroidal components of the magnetic field, and the other with dominant toroidal component. The two equilibria (denoted I and II below) are distinguished by different scaling of the physical variables with  $\epsilon$  which generally may be written as  $f(r, \zeta) = \epsilon^S \bar{f}(r, \zeta)$ . All equilibrium variables are written in the leading order in  $\epsilon$ , and depend on the radial variable only.

**Table 1.** Scales in  $\epsilon$  of the equilibrium variables for two types of equilibria (I) and (II).

$f = \epsilon^{\bar{S}} \bar{f}$	$n$	$V_r$	$V_\theta$	$V_z$	$B_r$	$B_\theta$	$B_z$	$j_r$	$j_\theta$	$j_z$	$E_r$	$E_\theta$	$E_z$
I, $\bar{S}$	0	> 1	0	> 2	> 1	0	0	> 1	0	0	0	> 1	> 1
II, $\bar{S}$	0	> 1	0	> 2	> 1	0	1	> 1	1	0	1	> 2	> 1

The exceptions are the number density and the pressure that depend on the axial coordinate in a self-similar manner with radius-dependent amplitude. The toroidal and axial magnetic fields as well as the disc thickness and the amplitude factor,  $\bar{N}(r)$ , in the number density are arbitrary functions of the radial variable. Those functions specify the equilibrium state.

To start the equilibrium description it is first assumed that both types of equilibria under the current study are characterized by a toroidal component of the magnetic field that is of order  $\epsilon^0$ . In contrast, in one equilibrium system (I) the axial component of the magnetic field is of order  $\epsilon^0$  as well, while in the other system (II) it is of order  $\epsilon$ . These assumptions together with relations (12)-(15), determine the order in  $\epsilon$  of the rest of the physical variables:

(I) *Comparable magnetic field components*

$$B_r = 0, \quad B_\theta = \epsilon^0 \bar{B}_\theta(r), \quad B_z = \epsilon^0 \bar{B}_z(r), \quad E_r = \epsilon^0 \bar{E}_r \equiv -\epsilon^0 \bar{V}_\theta(r) \bar{B}_z(r), \quad E_\theta = E_z = o(\epsilon),$$

$$j_r = o(\epsilon), \quad j_\theta = \epsilon^0 \bar{j}_\theta(r) \equiv -\epsilon^0 \frac{d\bar{B}_z}{dr}, \quad j_z = \epsilon^0 \bar{j}_z \equiv \epsilon^0 \frac{1}{r} \frac{d(r\bar{B}_\theta)}{dr}. \quad (16)$$

(II) *Dominant toroidal magnetic field*

$$B_r = 0, \quad B_\theta = \epsilon^0 \bar{B}_\theta(r, \zeta), \quad B_z = \epsilon \bar{B}_z(r), \quad E_r = \epsilon \bar{E}_r \equiv -\epsilon \bar{V}_\theta(r) \bar{B}_z(r), \quad E_\theta = E_z = o(\epsilon),$$

$$j_r = o(\epsilon), \quad j_\theta = \epsilon \bar{j}_\theta(r) \equiv -\epsilon \frac{d\bar{B}_z}{dr}, \quad j_z = \epsilon^0 \bar{j}_z \equiv \epsilon^0 \frac{1}{r} \frac{d(r\bar{B}_\theta)}{dr}. \quad (17)$$

For convenience the results are summarized in Table 1. It is noted finally that to lowest order in  $\epsilon$  the magnetic field configurations under consideration do not influence the steady-state properties of the disk. As will be seen in the following sections, this situation changes dramatically when small perturbations are considered.

### 2.3 Perturbed thin discs

In general for the unsteady nonlinear case the dependent variables are scaled in  $\epsilon$  in the following way:

$$f(r, \zeta, t) = \epsilon^{\bar{S}} \bar{f}(r, \zeta) + \epsilon^{S'} f'(r, \zeta, t). \quad (18)$$

Here  $f(r, \zeta, t)$  stands for any dependent variable, the bar and the prime denote equilibrium and perturbed variables; each perturbed variable is characterized by some power  $S'$  that is different for two types of equilibria I and II. The various cases are summarized in (Table 2).

## 3 DYNAMICAL EQUATIONS FOR THE PERTURBED DISC: TYPE I EQUILIBRIA

Consider first equilibria of type I, namely thin discs under the effect of a magnetic field with comparable poloidal and toroidal components.

### 3.1 The reduced nonlinear equations

Substituting (12)-(18) into (2) - (6) yields the following system of the reduced non-linear equations that governs the dynamical behavior of thin discs:

$$\frac{\partial V_r'}{\partial t} - 2\bar{\Omega}(r)V_\theta' + V_z' \frac{\partial V_r'}{\partial \zeta} - \frac{1}{\beta} \frac{\bar{B}_z(r)}{\bar{n} + n'} \frac{\partial B_r'}{\partial \zeta} = 0, \quad (19)$$

$$\frac{\partial V_\theta'}{\partial t} + \frac{1}{r} \frac{d(r^2 \bar{\Omega})}{dr} V_r' + V_z' \frac{\partial V_\theta'}{\partial \zeta} - \frac{1}{\beta} \frac{\bar{B}_z(r)}{\bar{n} + n'} \frac{\partial B_\theta'}{\partial \zeta} = 0, \quad (20)$$

$$\frac{\partial V_z'}{\partial t} + c_s^2(r) \frac{\bar{n}}{\bar{n} + n'} \frac{\partial}{\partial \zeta} \left( \frac{n'}{\bar{n}} \right) + \frac{1}{\beta} \bar{B}_\theta(r) \frac{\partial}{\partial \zeta} \left( \frac{B_\theta'}{\bar{n} + n'} \right) = -\frac{1}{2} \frac{\partial}{\partial \zeta} (V_z'^2 + \frac{1}{\beta} \frac{B_\theta'^2 + B_r'^2}{\bar{n} + n'}), \quad (21)$$

$$\frac{\partial n'}{\partial t} + \frac{\partial[(\bar{n} + n')V_z']}{\partial \zeta} = 0, \quad (22)$$

$$\frac{\partial B_r'}{\partial t} - \bar{B}_z(r) \frac{\partial V_r'}{\partial \zeta} = -\frac{\partial V_z' B_r'}{\partial \zeta}, \quad (23)$$

**Table 2.** Scales in  $\epsilon$  of the perturbed variables for two types of equilibria (I) and (II).

$f = \epsilon^{\bar{S}} \bar{f} + \epsilon^{S'} f'$	$n$	$V_r$	$V_\theta$	$V_z$	$B_r$	$B_\theta$	$B_z$	$j_r$	$j_\theta$	$j_z$	$E_r$	$E_\theta$	$E_z$
I, $S'$	0	1	1	1	0	1	1	-1	-1	0	1	1	0
II, $S'$	0	0	0	1	0	0	1	-1	-1	0	1	1	0

$$\frac{\partial B'_\theta}{\partial t} - \bar{B}_z(r) \frac{\partial V'_\theta}{\partial \zeta} - r \frac{d\bar{\Omega}}{dr} B'_r = - \frac{\partial V'_z B'_\theta}{\partial \zeta} - \bar{B}_\theta(r) \frac{\partial V'_z}{\partial \zeta}. \quad (24)$$

The system of equations (19) - (24) is subject to the boundary condition of least possible divergence for the axial velocity at infinity along with the conditions for the in-plane magnetic field as follows from (8)

$$B'_r = 0, \quad B'_\theta = 0 \quad \text{for} \quad \zeta = \pm\infty. \quad (25)$$

The equation for the perturbed axial magnetic field,  $B'_z$ , decouples from the rest equations, and drops out from the governing system of equations (19) - (24). Equation (21) has been derived with the help of the second steady-state relation (14). Furthermore, the radial derivatives drop out from the system of Eqs. (19) - (25). This, it should be stressed, is so not due to a frozen coefficients assumption, but is a direct result of the thin disc geometry. An important conclusion from the absence of radial derivatives in the reduced system of equations of the thin disc approximation is that transient non-exponential growth is not possible in such configuration. As will subsequently be shown (see Section 4 of the present paper), this picture changes dramatically when the dominant magnetic fields are toroidal, in which case the only possible axisymmetric instability is due to non-modal algebraic transient growth.

As the radial coordinate is a mere parameter in the set of the reduced equations, it is convenient to replace the physical variables by the following self-similar quantities:

$$\tau = t, \quad \eta = \frac{\zeta}{\bar{H}(r)}, \quad (26)$$

such that the derivatives in the new and old variables are related as follows:

$$\frac{\partial}{\partial t} = \frac{\partial}{\partial \tau}, \quad \frac{\partial}{\partial \zeta} = \frac{1}{\bar{H}(r)} \frac{\partial}{\partial \eta}. \quad (27)$$

Finally, system (19) - (25) may be written in a simpler form by introducing the following scaled dependent variables:

$$\mathbf{v}(\tau, r, \eta) = \frac{\mathbf{V}'}{\bar{c}_S(r)}, \quad \nu(\tau, r, \eta) = \frac{n'}{\bar{N}(r)}, \quad \mathbf{b}(\tau, r, \eta) = \frac{\mathbf{B}'}{\bar{B}_z(r)}. \quad (28)$$

Below for convenience and with no confusion the notation  $t$  for the time variable is reinstated instead of the new variable  $\tau$ . This yields the following system of equations that depend parametrically on the radius:

$$\frac{1}{\bar{\Omega}(r)} \frac{\partial v_r}{\partial t} - 2v_\theta - \frac{1}{\bar{\beta}_z(r)} \frac{1}{\bar{\nu}(\eta) + \nu} \frac{\partial b_r}{\partial \eta} = -v_z \frac{\partial v_r}{\partial \eta}, \quad (29)$$

$$\frac{1}{\bar{\Omega}(r)} \frac{\partial v_\theta}{\partial t} + \frac{1}{2} v_r - \frac{1}{\bar{\beta}_z(r)} \frac{1}{\bar{\nu}(\eta) + \nu} \frac{\partial b_\theta}{\partial \eta} = -v_z \frac{\partial v_\theta}{\partial \eta}, \quad (30)$$

$$\frac{1}{\bar{\Omega}(r)} \frac{\partial v_z}{\partial t} + \frac{\bar{\nu}(\eta)}{\bar{\nu}(\eta) + \nu} \frac{\partial}{\partial \eta} \left( \frac{\nu}{\bar{\nu}(\eta)} \right) + \frac{1}{\sqrt{\bar{\beta}_z(r) \bar{\beta}_\theta(r)}} \frac{\partial}{\partial \eta} \left[ \frac{b_\theta}{\bar{\nu}(\eta) + \nu} \right] = -\frac{1}{2} \frac{\partial}{\partial \eta} [v_z^2 + \frac{1}{\bar{\beta}_z(r)} \frac{b_\theta^2 + b_r^2}{\bar{\nu}(\eta) + \nu}], \quad (31)$$

$$\frac{1}{\bar{\Omega}(r)} \frac{\partial \nu}{\partial t} + \frac{\partial[(\bar{\nu}(\eta) + \nu)v_z]}{\partial \eta} = 0, \quad (32)$$

$$\frac{1}{\bar{\Omega}(r)} \frac{\partial b_r}{\partial t} - \frac{\partial v_r}{\partial \eta} = -\frac{\partial(v_z b_r)}{\partial \eta}, \quad (33)$$

$$\frac{1}{\bar{\Omega}(r)} \frac{\partial b_\theta}{\partial t} - \frac{\partial v_\theta}{\partial \eta} + \frac{3}{2} b_r = -\frac{\partial(v_z b_\theta)}{\partial \eta} - \sqrt{\frac{\bar{\beta}_z(r)}{\bar{\beta}_\theta(r)}} \frac{\partial v_z}{\partial \eta}, \quad (34)$$

supplemented by the boundary condition of least possible divergence for the axial velocity along with the vanishing conditions for the in-plane magnetic field at infinity. Here the Keplerian epicyclic frequency,  $\bar{\chi}(r) = \bar{\Omega}(r)$  has been employed;  $\bar{\nu}(\eta)$  is the scaled equilibrium density;  $\bar{\beta}_z(r)$  and  $\bar{\beta}_\theta(r)$  are the local axial and toroidal plasma beta functions:

$$\bar{\beta}_z(r) = \beta \frac{\bar{N}(r) \bar{c}_S^2(r)}{\bar{B}_z^2(r)}, \quad \bar{\beta}_\theta(r) = \beta \frac{\bar{N}(r) \bar{c}_S^2(r)}{\bar{B}_\theta^2(r)}, \quad (35)$$

where both local parameters  $\bar{\beta}_z(r)$  and  $\bar{\beta}_\theta(r)$  are proportional to the characteristic plasma beta,  $\beta$ .

Relations (29)-(35) form the full nonlinear MHD problem in the thin disc approximation and are named as defined above, the reduced nonlinear equations.

### 3.2 The linear problem.

Assuming now that the perturbations are small, the system of equations (29)-(34) may be linearized about the steady-state equilibrium solution. This yields:

$$\frac{1}{\bar{\Omega}(r)} \frac{\partial v_r}{\partial t} - 2v_\theta - \frac{1}{\bar{\beta}_z(r)\bar{\nu}(\eta)} \frac{\partial b_r}{\partial \eta} = 0, \quad (36)$$

$$\frac{1}{\bar{\Omega}(r)} \frac{\partial v_\theta}{\partial t} + \frac{1}{2}v_r - \frac{1}{\bar{\beta}_z(r)\bar{\nu}(\eta)} \frac{\partial b_\theta}{\partial \eta} = 0, \quad (37)$$

$$\frac{1}{\bar{\Omega}(r)} \frac{\partial b_r}{\partial t} - \frac{\partial v_r}{\partial \eta} = 0, \quad (38)$$

$$\frac{1}{\bar{\Omega}(r)} \frac{\partial b_\theta}{\partial t} - \frac{\partial v_\theta}{\partial \eta} + \frac{3}{2}b_r = -\sqrt{\frac{\bar{\beta}_z(r)}{\bar{\beta}_\theta(r)}} \frac{\partial v_z}{\partial \eta}, \quad (39)$$

$$\frac{1}{\bar{\Omega}(r)} \frac{\partial v_z}{\partial t} + \frac{\partial}{\partial \eta} \left( \frac{\nu}{\bar{\nu}(\eta)} \right) = -\frac{1}{\sqrt{\bar{\beta}_z(r)\bar{\beta}_\theta(r)}} \frac{\partial}{\partial \eta} \left[ \frac{b_\theta}{\bar{\nu}(\eta)} \right], \quad (40)$$

$$\frac{1}{\bar{\Omega}(r)} \frac{\partial \nu}{\partial t} + \frac{\partial [\bar{\nu}(\eta)v_z]}{\partial \eta} = 0. \quad (41)$$

To simplify the analysis, the equilibrium toroidal magnetic field is set to zero for type I equilibria, or equivalently,  $\bar{\beta}_\theta(r) = \infty$ . Under such conditions the reduced linearized system (36) - (41) is divided into two decoupled sub-systems that describe the dynamics of two different modes, namely: the Alfvén-Coriolis and the sound modes. In that case the characteristic magnetic field is specified as the dimensional axial component of the equilibrium magnetic field  $B_* = B_z(r_*)$ . It is indeed the approximation that is adopted in the remaining of the current analysis of type I equilibria.

### 3.3 Linear stability analysis for the Alfvén-Coriolis modes.

We start by representing the perturbations up to a radius-dependent amplitude factor as follows:

$$f(r, \eta, t) = \exp[-i\lambda(r)t] \hat{f}(r, \eta), \quad (42)$$

where  $\lambda(r)$  is the complex eigenvalue

$$\lambda = \Lambda + i\Gamma. \quad (43)$$

Substituting (42)-(43) into (36)-(41) results in the following system of linear ordinary differential equations for the perturbed velocity as well as in-plane magnetic field components. That system of equations characterizes the Alfvén-Coriolis waves and depends parametrically on the radius:

$$-i\lambda \hat{v}_r - 2\hat{v}_\theta - \frac{1}{\bar{\beta}_z(r)\bar{\nu}(\eta)} \frac{d\hat{b}_r}{d\eta} = 0, \quad (44)$$

$$-i\lambda \hat{v}_\theta + \frac{1}{2}\hat{v}_r - \frac{1}{\bar{\beta}_z(r)\bar{\nu}(\eta)} \frac{d\hat{b}_\theta}{d\eta} = 0, \quad (45)$$

$$-i\lambda \hat{b}_r - \frac{d\hat{v}_r}{d\eta} = 0, \quad (46)$$

$$-i\lambda \hat{b}_\theta - \frac{d\hat{v}_\theta}{d\eta} + \frac{3}{2}\hat{b}_r = 0. \quad (47)$$

In addition, the Alfvén-Coriolis sub-system (44)-(47) is subject to the vanishing boundary conditions for the in-plane magnetic-field components.

The linear set of equations (44)-(47) may be reduced to the following single fourth order ordinary differential equations for both  $\hat{b}_r$  and  $\hat{b}_\theta$ :

$$\frac{d}{d\eta} \left[ \frac{1}{\bar{\nu}(\eta)} \frac{d^2}{d\eta^2} \left( \frac{1}{\bar{\nu}(\eta)} \frac{d\hat{b}_{r,\theta}}{d\eta} \right) \right] + \bar{\beta}_z(r)(3 + 2\lambda^2) \frac{d}{d\eta} \left( \frac{1}{\bar{\nu}(\eta)} \frac{d\hat{b}_{r,\theta}}{d\eta} \right) + \bar{\beta}_z^2(r)\lambda^2(\lambda^2 - 1)\hat{b}_{r,\theta} = 0. \quad (48)$$

Equation (48) is the same as the one used by Liverts & Mond (2009) who have derived it for a model problem under the assumption of zero radial variations of the perturbations. Here, it is important to emphasize however that the radial coordinate is a parameter a fact that renders the radial dependence of the perturbations arbitrary. Liverts & Mond (2009) have solved (48) with the aid of the Wentzel-Kramers-Brillouin (WKB) approximation. Remarkably, however, that a full analytical solution of Eq. (48) is possible for a slightly modified density profile. The first and main step towards that goal is to replace the isothermal density vertical steady-state distribution  $\bar{\nu}(\eta) = \exp(-\eta^2/2)$  by the following function:

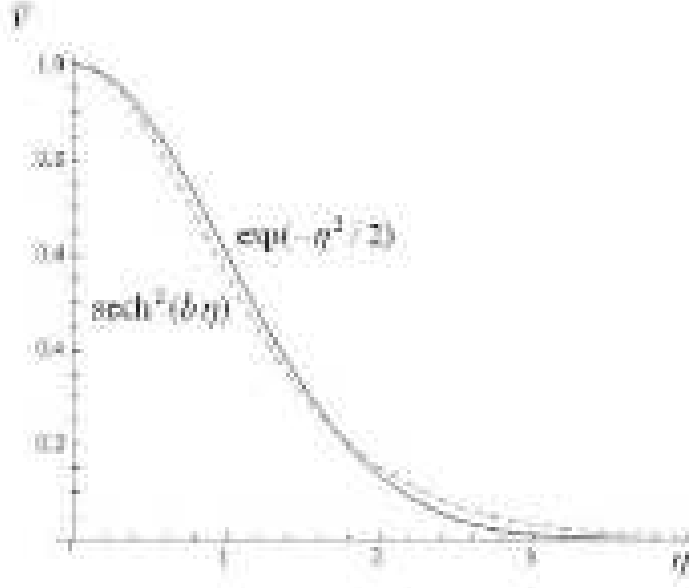


**Figure 1.** The comparison of true,  $\bar{\nu} = \exp(-\eta^2/2)$  (solid) and model,  $\bar{\nu} = \text{sech}^2(b\eta)$  (dashed) number density profiles;  $b = \sqrt{2/\pi}$ .

$$\bar{\nu}(\eta) = \text{sech}^2(b\eta), \quad (49)$$

where the shape parameter  $b$  is determined by the requirement that the total mass of the disc does not change, namely:

$$\int_0^\infty \exp(-\eta^2/2) d\eta = \int_0^\infty \text{sech}^2(b\eta) \eta. \quad (50)$$

The result is:

$$b = \sqrt{2/\pi}. \quad (51)$$

The comparison of true and model number density profiles is presented in Fig. 1 and demonstrates a close correspondence between them. Furthermore, it will be shown below that the results derived by employing that profile are practically indistinguishable from the WKB results obtained for the true exponential distribution. In fact, notwithstanding the use of the terms true and model profiles, such a change of the equilibrium profile of the number density (that is determined by the axial momentum balance equation) may actually represent some true equilibrium that is obtained from a slightly different gravitational potential [see Spitzer (1942), where a similar density profile has been obtained as an exact solution for flat disc-galaxies whose disc mass content is larger than the mass of the central object].

Instead of Eq. (48) for the perturbed magnetic field it is more convenient to consider the equation for the perturbed velocity. Thus, substituting (49) - (51) into (44) - (47), yields the following ordinary differential equations for  $\hat{v}_r$  and  $\hat{v}_\theta$ :

$$\frac{1}{\bar{\nu}(\eta)} \frac{d^2}{d\eta^2} \left( \frac{1}{\bar{\nu}(\eta)} \frac{d^2 \hat{v}_{r,\theta}}{d\eta^2} \right) + \bar{\beta}_z (3 + 2\lambda^2) \frac{1}{\bar{\nu}(\eta)} \frac{d^2 \hat{v}_{r,\theta}}{d\eta^2} + \bar{\beta}_z^2 \lambda^2 (\lambda^2 - 1) \hat{v}_{r,\theta} = 0. \quad (52)$$

The next step now is to introduce a new independent variable  $\xi = \tanh(b\eta)$ , such that  $-1 \leq \xi \leq 1$ . Doing that, a simpler equation emerges, which may be cast into the following form:

$$(L + K^-)(L + K^+) \hat{v}_\theta = 0, \quad (53)$$

where  $L$  is the Legendre operator of second order:

$$L = \frac{d}{d\xi} [(1-\xi^2) \frac{d}{d\xi}], \quad K^\pm = \frac{\bar{\beta}_z}{2b^2} [3 + 2\lambda^2 \pm \sqrt{9 + 16\lambda^2}].$$

Imposing now the zero boundary conditions of  $\hat{b}_\theta$  at  $\eta \rightarrow \infty$  leads to the requirement that the solution of Eq. (53) for  $\hat{v}_\theta$  diverges polynomially at most when  $\eta \rightarrow \infty$ . It is concluded therefore that  $\hat{v}_\theta$  is proportional to the Legendre polynomials  $P_k(\xi)$  which are the solutions of the following equation:

$$\frac{d}{d\xi} \left( (1-\xi^2) \frac{dP_k}{d\xi} \right) + K^\pm P_k, \quad K^\pm = k(k+1), \quad k = 1, 2, \dots \quad (54)$$

Thus, the eigenvalues  $\lambda^\pm$  are now determined by the dispersion relation

$$K^\pm \equiv \frac{\bar{\beta}_z(r)}{2b^2} [3 + 2\lambda^2 \pm \sqrt{9 + 16\lambda^2}] = k(k+1). \quad (55)$$

Employing now the recursive relations for the Legendre polynomials:

$$(1-\xi^2) \frac{dP_k}{d\xi} = \frac{k(k+1)}{2k+1} [P_{k-1}(\xi) - P_{k+1}(\xi)],$$

setting the arbitrary amplitude of  $\hat{v}_\theta$  to unity, and using the linear equations (44) - (47) result in the following expressions for the eigenfunctions that are determined up to an arbitrary radius dependent amplitude factor:

$$\begin{aligned} \hat{v}_r^\pm &= i\lambda_a^\pm \left( \frac{1}{2} + \frac{3}{2} \frac{1}{\hat{\beta}_z} \frac{\hat{\beta}_z - 1}{(\lambda_a^\pm)^2} \right) P_k(\xi), \quad \hat{v}_\theta^\pm = P_k(\xi), \\ \hat{b}_r^\pm &= \frac{k(k+1)}{2k+1} \frac{b}{6} [(\lambda_a^\pm - 1)(\lambda_a^\pm + 1)\hat{\beta}_z - 3] [P_{k-1}(\xi) - P_{k+1}(\xi)], \\ \hat{b}_\theta^\pm &= \frac{k(k+1)}{2k+1} \frac{b}{4} \frac{(1 - \lambda_a^\pm)(\lambda_a^\pm + 1)\hat{\beta}_z - 1}{i\lambda_a^\pm} [P_{k-1}(\xi) - P_{k+1}(\xi)], \end{aligned} \quad (56)$$

where  $k = 1, 2, \dots$  plays the role of axial wave number,  $\hat{b}_\theta^\pm = 0$  for  $\xi = \pm 1$ , since  $P_k(1) = 1$  and  $P_k(-1) = (-1)^k$  for all  $k$ .

Turning back to the dispersion relation (58), it may be written as follows:

$$(\lambda^\pm)^4 \hat{\beta}_z^2 - (\lambda^\pm)^2 \hat{\beta}_z (\hat{\beta}_z + 6) + 9(1 - \hat{\beta}_z) = 0, \quad \hat{\beta}_z = \frac{\bar{\beta}_z}{\bar{\beta}_{cr}^{(k)}}. \quad (57)$$

It is thus obvious that the  $k$ -th mode is destabilized when the beta value crosses from below the threshold that is given by:

$$\bar{\beta}_{cr}^{(k)} = \frac{2}{3\pi} k(k+1). \quad (58)$$

As a result, a universal (for all values of  $\bar{\beta}_z(r)$  and  $k$ ) criterion for instability emerges which reads:  $\hat{\beta}_z(r) > 1$ . Written in terms of the scaled plasma beta  $\hat{\beta}_z$  the dispersion relation (57) has the following solutions for the eigenvalues of the Alfvén-Coriolis modes (see Fig. 1):

$$\lambda^\pm = \sqrt{\frac{\hat{\beta}_z + 6 \pm \sqrt{(\hat{\beta}_z + 6)^2 - 36(1 - \hat{\beta}_z)}}{2\hat{\beta}_z}}. \quad (59)$$

The two eigenvalues,  $\lambda^+$  and  $\lambda^-$ , represent fast and slow Alfvén-Coriolis waves. While the fast Alfvén-Coriolis modes are always stable, the number of unstable slow modes signified by the plasma beta. The eigenvalues of the slow Alfvén-Coriolis modes,  $\lambda^-$ , are given therefore by:

$$\begin{aligned} \lambda^- &= \Lambda_a^- = \pm \sqrt{\frac{\hat{\beta}_z + 6 - \sqrt{(\hat{\beta}_z + 6)^2 - 36(1 - \hat{\beta}_z)}}{2\hat{\beta}_z}}, \quad \text{Im}\{\lambda^-\} = 0 \quad \text{for } \hat{\beta}_z \leq 1, \\ \lambda^- &= i\Gamma_a^- = \pm i \sqrt{\frac{\sqrt{(\hat{\beta}_z + 6)^2 + 36(\hat{\beta}_z - 1)} - \hat{\beta}_z - 6}{2\hat{\beta}_z}}, \quad \text{Re}\{\lambda^-\} = 0 \quad \text{for } \hat{\beta}_z > 1. \end{aligned} \quad (60)$$

The eigenvalues are imaginary, and the system is spectrally unstable if  $\hat{\beta}_z > 1$ , and real for  $\hat{\beta}_z < 1$  in which case the system is stable. In particular, the minimal critical unscaled plasma beta that is needed for instability is determined by the first unstable slow Alfvén-Coriolis mode,  $k = 1$ , and is given by  $\bar{\beta}_{cr}^{(1)} = 0.42$ . The unstable modes are the well known MRIs and from Eq. (58) it is easy to calculate how many of them are excited for a given value of the plasma beta. Thus, there are  $k$  unstable modes for  $\bar{\beta}_{cr}^{(1)} \leq \bar{\beta}_z(r) \leq \bar{\beta}_{cr}^{(k+1)}$ . In particular, Eq. (58) yields approximately the square-root law for the number of the unstable modes vs plasma beta:

$$k < \sqrt{3\pi \bar{\beta}_z(r)/2}. \quad (61)$$

Relation (58) or its simplified version (61) is significant for the consequent modeling of non-linear development of the instability. It is finally emphasized that the stability criterion as well as the number of unstable modes depend on the radius. Thus, different areas within the disc may be characterized by different stability properties as well as different number of unstable modes.

The family of the fast Alfvén-Coriolis modes,  $\lambda^+(\hat{\beta}_z)$ , is characterized by the frequencies that are much larger than the Keplerian frequency for small values of the scaled plasma beta (large values of axial wave number or small plasma beta) and tends to the Keplerian value at large plasma beta values:



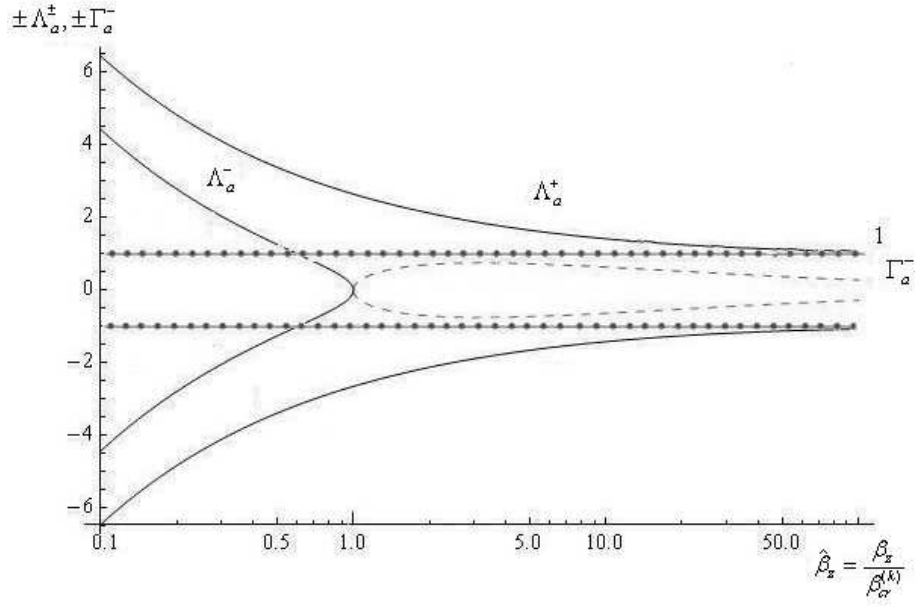


**Figure 2.** Growth rates  $\pm\Gamma_a^-$  (dashed lines) for the unstable Alfvén-Coriolis (MRI) modes and frequencies  $\pm\Lambda_a^\pm$  (solid lines) for the Alfvén-Coriolis oscillations vs universal scaled plasma beta,  $\hat{\beta}_z = \bar{\beta}_z(r)/\bar{\beta}_{cr}^{(k)}$ ,  $\bar{\beta}_{cr}^{(k)} = 2k(k+1)/(3\pi)$  for the model number density  $\bar{\nu} = \text{sech}^2(\sqrt{2/\pi}\eta)$ ;  $k = 1, 2, \dots$  is the axial wave number. Meshed straight-line asymptotes at  $\hat{\beta}_z \gg 1$  are the scaled Keplerian frequencies,  $\pm\Lambda_a^\pm = \pm 1$ .

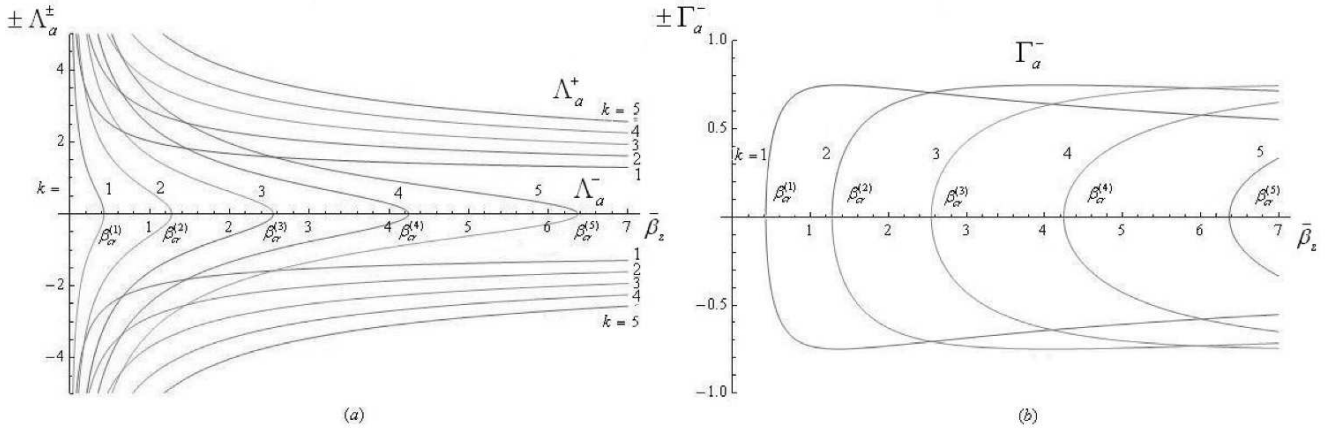


**Figure 3.** Frequencies  $\pm\Lambda_a^\pm$  for the first five fast and slow Alfvén-Coriolis modes and growth rates  $\pm\Gamma_a^-$  for the unstable (MRI) slow Alfvén-Coriolis modes vs ununscaled plasma beta  $\bar{\beta}_z$  for the model number density  $\bar{\nu} = \text{sech}^2(\sqrt{2/\pi}\eta)$ ;  $\bar{\beta}_{cr}^{(k)} = 2k(k+1)/(3\pi)$  is the critical plasma beta,  $k = 1, 2, 3, 4, 5$  is the axial wave number.

$$\lambda^+ = \Lambda_a^+ = \pm \sqrt{\frac{\hat{\beta}_z + 6 + \sqrt{(\hat{\beta}_z + 6)^2 - 36(1 - \hat{\beta}_z)}}{2\hat{\beta}_z}}, \quad \text{Im}\{\lambda^+\} = 0. \quad (62)$$

Expressed in terms of the scaled plasma beta, a single figure depicts all possible stable as well as unstable modes. This is shown in Fig. 2. The maximal growth rate for the unstable modes is achieved around  $\hat{\beta}_z \approx 3$ , which for a given plasma beta value determines the axial wave number of the fastest growing modes.

Frequencies and growth rates for the first five fast and slow Alfvén-Coriolis modes are presented in Fig. 3 (in terms of the ununscaled beta,  $\bar{\beta}_z$ ). The corresponding growth rates  $\Gamma_a^-$  obtained by Liverts & Mond (2009) by employing the WKB approximation are practically indistinguishable from those in Fig. 3 and therefore are not shown on the figure. In particular, the critical plasma beta  $\bar{\beta}_{cr}^{(1)}$  found by Liverts & Mond (2009) (after correction by factor 2 due to the different definition of the plasma beta there) is 0.417, which is practically the same as the one obtained in the current work.

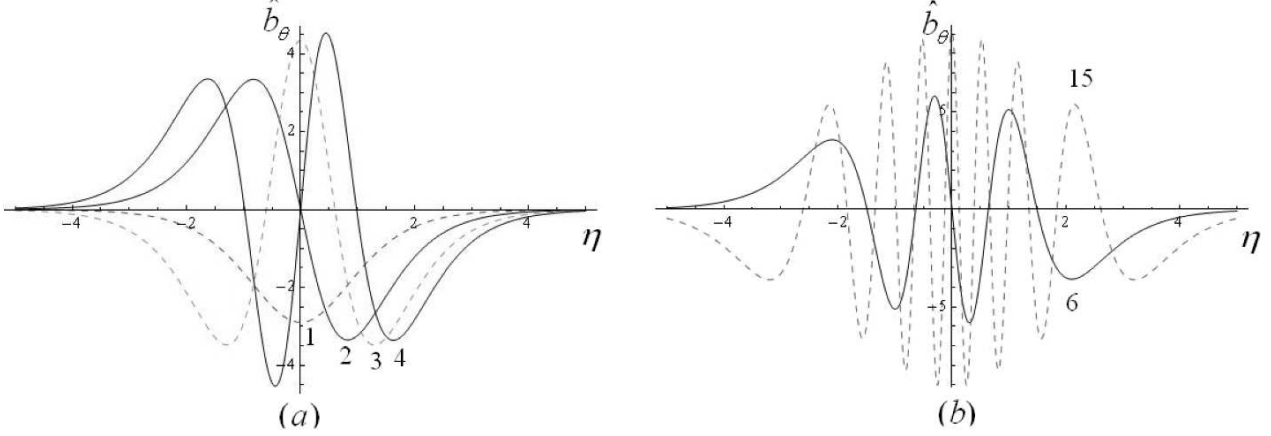


**Figure 4.** The toroidal component of the perturbed magnetic field  $\hat{b}_\theta$  vs self-similar axial variable  $\eta = z/H(r)$  for the Legendre polynomials with the axial wave numbers (a)  $k = 1, 2, 3, 4$  and (b)  $k = 6, 15$ . All curves are calculated for the fixed value of  $\hat{\beta}_z = 1.5$  ( $\hat{\beta}_z = \bar{\beta}_z/\bar{\beta}_{cr}^{(k)}$ ,  $\bar{\beta}_{cr}^{(k)} = b^2 k(k+1)/3$ , dashed and solid curves correspond to the odd and even  $k$ , respectively).

**Table 3.** Distances of the turning points from the midplane vs axial wave number.

$k$	1	2	3	4	5	6	15	35	155	1555
$\eta_*$	1.18	1.89	2.23	2.45	2.6	2.7	3.3	3.78	4.5	5.42

An illustration of the perturbed toroidal magnetic field is presented in Fig. 4. The perturbations are indeed localized within the effective height of the disc which weakly depends on the axial wave number. This corresponds to a finite distance between the turning points – the natural characteristics of the problem solution in the WKB approximation [Liverts & Mond (2009)]. To explicitly demonstrate the finite size of the region of perturbation’s location, the differential equation for the perturbed magnetic field  $\hat{b}_\theta$  in the self - similar variable  $\eta$  is written out:

$$\frac{d^2 \hat{b}_\theta}{d\eta^2} + 2b\xi \frac{d\hat{b}_\theta}{d\eta} + b^2 K^\pm (1 - \xi^2) \hat{b}_\theta = 0, \quad \xi = \tanh(b\eta), \quad b = \sqrt{\frac{2}{\pi}}, \quad K^\pm = k(k+1), \quad k = 1, 2, \dots, \quad (63)$$

which is subject to zero boundary conditions at infinity. Equation (63) is derived by using differential equation (53) for  $\hat{v}_\theta$  and a fact that  $\hat{b}_\theta$  up to a constant coefficient of proportionality is equal to  $d\hat{v}_\theta/d\eta$ . Transforming as in WKB approximation the dependent variable  $\hat{b}_\theta = Q(\eta) \int \mu(\eta) d\eta$ , and setting  $\mu(\eta) = -\xi = -\tanh(b\eta)$  in order to eliminate terms with first order derivatives yield:

$$\frac{d^2 Q}{d\eta^2} + \varkappa^2(\eta) Q = 0, \quad \varkappa^2(\eta) = b^2 [K^\pm (1 - \xi^2) - 1]. \quad (64)$$

Then the turning points are determined from the relation  $\varkappa^2(\eta) = 0$ , and may be found explicitly substituting  $1 - \xi^2$  by equivalent expression  $\exp(-\eta^2/2)$ :

$$\eta_* = \pm \sqrt{2 \ln[k(k+1)]}, \quad k = 1, 2, \dots \quad (65)$$

The results for several axial wave numbers are presented in Table 3. Although the oscillation’s region unboundedly expanded with rising axial wave numbers, this occurs very slowly and the region has relatively low sizes even at high values of  $k$ . Note that the unbounded growth which corresponds to high wave numbers should be suppressed by dissipative effects neglected in the present analysis.

In order to compare the current results to well known results for infinite homogeneous cylinders Balbus & Hawley (1991) the growth rate of the unstable modes is depicted in Fig. 5 as a function of the axial wave number  $K$ , where

$$K = k \frac{L_a}{H\sqrt{2}} \equiv \frac{k}{\sqrt{2\beta_z}}, \quad (66)$$

$L_a = V_a/\Omega$  is the Alfvén length scale,  $z = H\sqrt{2}$  is the effective height of the diffused disc at which the equilibrium number density,  $\bar{n} \sim \exp[-z^2/(2H^2)]$ , falls by factor  $e^{-1}$ . The effective wave number  $K$  is the discrete thin-disc analog of the continuous wave number for infinite cylindrical discs. For fixed value of the local plasma beta,  $\bar{\beta}_z = 0.41, 0.5, 1.5, 2.5, 500$ , the discrete set of the points in the plane  $\{K, \Gamma_a^-\}$  is presented by one of the interpolating curves 1, 2, 3, 4, 5, respectively. The number of the discrete points on each interpolating curves corresponds to the admissible values of the Alfvén-Coriolis mode number  $k = 1, 2, 3, \dots$  for which  $\bar{\beta}_{cr}^{(1)} \leq \bar{\beta}_{cr}^{(k)} \leq \bar{\beta}_z(r)$ . Also, the range of unstable  $k$ -values is widening as the value of  $\bar{\beta}_z$  is increased.

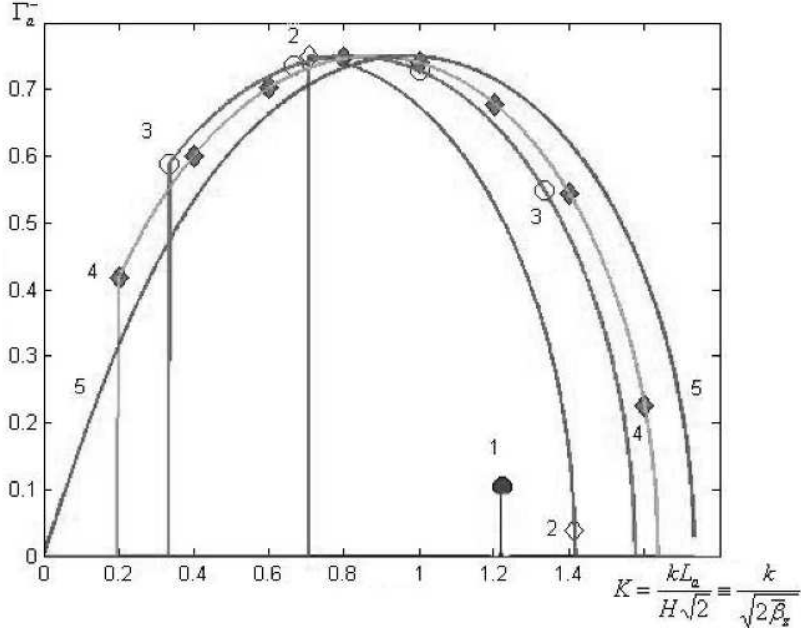


**Figure 5.** Growth rates  $\Gamma_a^-$  for the slow Alfvén-Coriolis modes vs effective wave number  $K = \frac{kL_a}{H\sqrt{2}} \equiv \frac{k}{\sqrt{2\beta_z}}$ ,  $k = 1, 2, 3, \dots$  is the number of the Alfvén-Coriolis modes, calculated for the model number density  $\bar{\nu} = \text{sech}(b\eta)$ . Interpolating curves 1, 2, 3, 4, 5 correspond to  $\bar{\beta}_z = 0.41, 0.71, 1.5, 2.5, 500$ , respectively.

In particular, at large plasma beta the corresponding set of the points due to their large number (curve 5) should tend to the continuous curve for infinite cylinder geometry in Balbus & Hawley (1991). For finite plasma beta there is a discrete number of points on each curves in Fig. 5, where the left bound corresponds to the first Alfvén-Coriolis mode,  $k = 1$ . Thus, for beta values close to  $\bar{\beta}_{cr}^{(1)}$ , the number of unstable modes is small and the disk stability properties significantly deviate from those predicted by the infinite cylinder model.

### 3.4 Linear stability problem for magnetosonic modes

For simplicity it is assumed now that the toroidal component of the equilibrium magnetic field is zero and hence  $\bar{\beta}_z = \infty$ . Thus, substituting the exponential ansatz (42) into Eqs. (40) - (41) for the magnetosonic modes, and assuming that their frequencies are different from the eigenvalues of inertial-Coriolis waves yields:

$$-i\lambda\hat{v}_z + \frac{d}{d\eta}\left[\frac{\hat{v}}{\bar{\nu}(\eta)}\right] = 0, \quad (67)$$

$$-i\lambda\frac{\hat{v}}{\bar{\nu}(\eta)} + \frac{d\hat{v}_z}{d\eta} - \eta\hat{v}_z = 0. \quad (68)$$

Since the effect of the magnetic field is dropped from the linear system (67) - (68), the latter actually describes sound waves that propagate vertically in the non-homogeneous disc. Eliminating the perturbed number density from (67) - (68) and substituting the equilibrium number density,  $\bar{\nu}(\eta) = \exp(-\eta^2/2)$ , in the resulting equation yields a second order differential equation for the perturbed axial velocity:

$$\frac{d^2\hat{v}_z}{d\eta^2} - \eta\frac{d\hat{v}_z}{d\eta} + (\lambda^2 - 1)\hat{v}_z = 0. \quad (69)$$

Equation (69) is the Hermite equation and the requirement that its solutions diverges polynomially at most when  $\eta \rightarrow \pm\infty$  determines the eigenvalues to be:

$$\lambda = \pm\Lambda_S = \pm\sqrt{m+1}, \quad (70)$$

while the eigenfunctions are given up to an amplitude factor depending on radius by:

$$\hat{v}_z = \mp i\sqrt{m+1}H_m(\eta), \quad \hat{v} = e^{-\eta^2/2}H_{m+1}(\eta). \quad (71)$$

Here  $H_m(\eta)$  ( $m = 1, 2, \dots$ ) are the Hermite polynomials. The axial velocities are polynomially unbounded functions at  $\eta \rightarrow \pm\infty$ . Note that now the number of the Hermite polynomial  $m$  plays the role of the axial wave number for the magnetosonic mode that

is different from the Alfvén-Coriolis modes with the number of the Legendre polynomial as the axial wave number. Formally, the above family of the solutions of the eigenvalue problem should be completed by the following degenerate steady-state solution:

$$\hat{v} = e^{-\eta^2/2}, \quad \hat{v}_z = 0. \quad (72)$$

However, the latter may be considered as a modification of the unperturbed equilibrium solution.

#### 4 DYNAMICAL EQUATIONS FOR PERTURBED THIN DISCS: TYPE II EQUILIBRIA

Consider now the thin disc problem under the effect of a dominant toroidal component of the equilibrium magnetic fields (see Tables 1 and 2). The solutions of such problem in the pure hydrodynamic case of zero magnetic field for adiabatic thin discs have been obtained and discussed in Shtemler et al. (2010) and are extended here for locally isothermal magnetized discs.

##### 4.1 The reduced nonlinear equations

At this stage it is convenient to rescale all the physical variables,  $f$ , with the small parameter  $\epsilon$ , without splitting the solution to its equilibrium and perturbed constituents. Thus, in a most general way, the physical variables are given by:

$$f(r, \zeta, t) = \epsilon^{S'} \tilde{f}(r, \zeta, t). \quad (73)$$

Here the auxiliary variables denoted by tilde are introduced, and the same orders,  $S'$ , in  $\epsilon$  are assumed for the physical variables as for the disturbed variables. For the dominant toroidal equilibrium magnetic field such choice is justified by the fact that any disturbed dependent variable is of the order of or larger than the corresponding equilibrium variable i.e.  $S' \leq \bar{S}$  (see Tables 1 and 2). This imposes an additional limitation on the admissible time of perturbation growth. Substituting (73) into (2) - (6) yields up to the terms of the higher order in  $\epsilon$  the following in-plane components of the momentum equation:

$$\frac{\partial \tilde{V}_r}{\partial t} + \tilde{V}_r \frac{\partial \tilde{V}_r}{\partial r} + \tilde{V}_z \frac{\partial \tilde{V}_r}{\partial \zeta} - \frac{\tilde{V}_\theta^2}{r} = -\frac{d\tilde{\Psi}}{dr}, \quad (74)$$

$$\frac{\partial \tilde{V}_\theta}{\partial t} + \tilde{V}_r \frac{\partial \tilde{V}_\theta}{\partial r} + \tilde{V}_z \frac{\partial \tilde{V}_\theta}{\partial \zeta} + \frac{\tilde{V}_r \tilde{V}_\theta}{r} = 0, \quad (75)$$

$$\frac{\partial \tilde{V}_z}{\partial t} + \tilde{V}_r \frac{\partial \tilde{V}_z}{\partial r} + \tilde{V}_z \frac{\partial \tilde{V}_z}{\partial \zeta} = -\frac{c_S^2}{\tilde{n}} \frac{\partial \tilde{n}}{\partial \zeta} - \frac{\partial \tilde{\psi}}{\partial \zeta} - \frac{1}{2\beta \tilde{n}} \frac{\partial (\tilde{B}_\theta^2 + \tilde{B}_r^2)}{\partial \zeta}, \quad (76)$$

$$\frac{\partial \tilde{n}}{\partial t} + \frac{1}{r} \frac{\partial (r \tilde{n} \tilde{V}_r)}{\partial r} + \frac{\partial (\tilde{n} \tilde{V}_z)}{\partial \zeta} = 0, \quad (77)$$

$$\frac{\partial \tilde{B}_r}{\partial t} + \frac{\partial \tilde{E}_\theta}{\partial \zeta} = 0, \quad (78)$$

$$\frac{\partial \tilde{B}_\theta}{\partial t} + \frac{\partial \tilde{E}_r}{\partial \zeta} - \frac{\partial \tilde{E}_z}{\partial r} = 0, \quad (79)$$

$$\frac{\partial \tilde{B}_z}{\partial t} + \frac{1}{r} \frac{\partial (r \tilde{E}_r)}{\partial r} = 0. \quad (80)$$

Here

$$\tilde{E}_r = \tilde{V}_z \tilde{B}_\theta - \tilde{V}_\theta \tilde{B}_z, \quad \tilde{E}_\theta = \tilde{V}_r \tilde{B}_z - \tilde{V}_z \tilde{B}_r, \quad \tilde{E}_z = \tilde{V}_\theta \tilde{B}_r - \tilde{V}_r \tilde{B}_\theta. \quad (81)$$

The system (74) - (81) is subject the boundary conditions at infinity of least possible divergence for the axial velocity and the vanishing of the in-plane magnetic-field components.

##### 4.2 The linearized problem

We start by linearizing the MHD equations (74) - (81) about the steady-state equilibrium solution (12) - (15). Substituting the decomposition of the total disturbed variables (18) into Eqs. (74) - (81), yields the following linear set of equations for axisymmetric perturbations:

$$\frac{\partial V'_r}{\partial t} - 2\bar{\Omega}(r)V'_\theta = 0, \quad (82)$$

$$\frac{\partial V'_\theta}{\partial t} + \frac{1}{2}\bar{\Omega}(r)V'_r = 0, \quad (83)$$

and

$$\frac{\partial V'_z}{\partial t} + \bar{c}_s^2(r) \frac{\partial}{\partial \zeta} \left( \frac{n'}{\bar{n}} \right) + \frac{1}{\beta} \frac{\bar{B}_\theta(r)}{\bar{n}} \frac{\partial B'_\theta}{\partial \zeta} = 0, \quad (84)$$

$$\frac{\partial n'}{\partial t} + \frac{\partial(\bar{n}V'_z)}{\partial \zeta} = -\frac{1}{r} \frac{\partial(r\bar{n}V'_r)}{\partial r}, \quad (85)$$

$$\frac{\partial B'_r}{\partial t} = \bar{B}_z(r) \frac{\partial V'_r}{\partial \zeta}, \quad (86)$$

$$\frac{\partial B'_\theta}{\partial t} + \bar{B}_\theta(r) \frac{\partial V'_z}{\partial \zeta} = r \frac{d\bar{\Omega}}{dr} B'_r + \bar{B}_z(r) \frac{\partial V'_\theta}{\partial \zeta} - \frac{\partial[\bar{B}_\theta(r)V'_r]}{\partial r}. \quad (87)$$

The equation for the perturbed axial magnetic field,  $B'_z$ , decouples from the rest of the equations, and drops out altogether from the governing system (82)-(87). As in the case of comparable axial and toroidal magnetic field components (type I equilibria), also the reduced linear system (82)-(87) is decoupled into two linear sub-systems that describe now the dynamics of the inertial-Coriolis (IC),  $\{V'_r, v'_\theta\}$ , and magnetosonic (MS),  $\{V'_z, n', B'_r, B'_\theta, B'_z\}$ , modes. A notable difference between the two cases however is that, while for the type I equilibria the radial derivatives drop out altogether from the reduced nonlinear system of equations, in the current case, some of the radial derivatives do survive the asymptotic procedure, due to the relative smallness of the axial magnetic field component. As will be shown later on, this difference turns out to be quite significant as the radial derivatives are responsible for the non modal algebraic growth of the initially small perturbations.

Back to the modes of wave propagation, the IC waves are described by Eqs. (82) and (83) while the MS modes are given by the solution of the homogeneous parts of Eqs. (84)-(87). Also, the perturbed radial magnetic field,  $B'_r$ , is completely determined by the perturbed radial velocity,  $V'_r$ , and hence Eq. (86) is separated from the rest of the magnetosonic sub-system. The right hand sides of Eqs. (85) and (87) result in the (resonant as well as nonresonant) forcing of the MS waves by the IC modes. As will be seen later on, this occurs due to the rotational shear.

Before actually solving the above linearized system of equations it is noted that, guided by the steady-state solution, it is convenient to introduce the following new independent variables:

$$\theta = t, \quad \rho = r, \quad \eta = \frac{\zeta}{\bar{H}(r)}, \quad (\bar{H}(r) = \frac{\bar{c}_s(r)}{\bar{\Omega}(r)}). \quad (88)$$

Then derivatives in new and old variables are related as follows:

$$\frac{\partial}{\partial t} = \frac{\partial}{\partial \theta}, \quad \frac{\partial}{\partial \zeta} = \frac{1}{\bar{H}} \frac{\partial}{\partial \eta}, \quad \frac{\partial}{\partial r} = \frac{\partial}{\partial \rho} - \frac{1}{\bar{H}^2} \frac{d\bar{H}}{d\rho} \eta \frac{\partial}{\partial \eta}. \quad (89)$$

Equations (82)-(87) may be rewritten by introducing the following scaled variables:

$$\mathbf{v}(\rho, \eta, \theta) = \frac{\mathbf{V}'}{\bar{c}_s(r)}, \quad \nu(\rho, \eta, \theta) = \frac{n'}{\bar{N}(r)}, \quad \mathbf{b}(\rho, \eta, \theta) = \frac{\mathbf{B}'}{\bar{B}_\theta(r)}. \quad (90)$$

Below for convenience and with no confusion we revert to the notation  $t$  for the new variable  $\tau$ . This yields the following system of equations:

$$\frac{1}{\bar{\Omega}} \frac{\partial v_r}{\partial t} - 2v_\theta = 0, \quad (91)$$

$$\frac{1}{\bar{\Omega}} \frac{\partial v_\theta}{\partial t} + \frac{1}{2}v_r = 0, \quad (92)$$

and

$$\frac{1}{\bar{\Omega}} \frac{\partial v_z}{\partial t} + \frac{\partial}{\partial \eta} \left[ \frac{\nu}{\bar{\nu}(\eta)} \right] + \frac{1}{\bar{\beta}_\theta \bar{\nu}(\eta)} \frac{\partial b_\theta}{\partial \eta} = 0, \quad (93)$$

$$\frac{1}{\bar{\Omega}} \frac{\partial}{\partial t} \left[ \frac{\nu}{\bar{\nu}(\eta)} \right] + \frac{\partial v_z}{\partial \eta} - \eta v_z = -\frac{\partial v_r}{\partial \rho} - \bar{D}_N v_r + \bar{D}_\Omega \left( \frac{\partial v_r}{\partial \eta} - \eta v_r \right) \eta, \quad (94)$$

$$\frac{1}{\bar{\Omega}} \frac{\partial b_r}{\partial t} = \sqrt{\frac{\bar{\beta}_\theta}{\bar{\beta}_z}} \frac{\partial v_r}{\partial \eta}, \quad (95)$$

$$\frac{1}{\bar{\Omega}} \frac{\partial b_\theta}{\partial t} + \frac{\partial v_z}{\partial \eta} = -\frac{\partial v_r}{\partial \rho} - \frac{3}{2}b_r + \sqrt{\frac{\bar{\beta}_\theta}{\bar{\beta}_z}} \frac{\partial v_\theta}{\partial \eta} - \bar{D}_B v_r + \bar{D}_\Omega \frac{\partial v_r}{\partial \eta} \eta. \quad (96)$$

Here  $\bar{\beta}_\theta(\rho)$  and  $\bar{\beta}_z(\rho)$  are given by (35) and are proportional to the characteristic plasma beta,  $\beta$ , that is now based on the dimensional toroidal component of the equilibrium magnetic field as the characteristic scale,  $B_* = B_\theta(r_*)$ ;  $\bar{D}_N(\rho)$ ,  $\bar{D}_\Omega(\rho)$  and  $\bar{D}_B(\rho)$  are the following logarithmic derivatives:

$$\bar{D}_N = \frac{d \ln(\bar{c}_S \bar{N})}{d\rho}, \quad \bar{D}_\Omega = \frac{d \ln(\bar{c}_S / \bar{\Omega})}{d\rho} \equiv \frac{d \ln \bar{H}}{d\rho}, \quad \bar{D}_B = \frac{d \ln(\bar{c}_S \bar{B}_\theta)}{d\rho}. \quad (97)$$

A single equation for the magnetosonic modes may be derived now by eliminating the toroidal component of the perturbed magnetic field as well as the perturbed number density from Eqs. (93) - (96). The result is:

$$\frac{1}{\Omega^2} \frac{\partial^2 v_z}{\partial t^2} - \left(1 + \frac{1}{\bar{\beta}_\theta \bar{\nu}(\eta)}\right) \frac{\partial^2 v_z}{\partial \eta^2} + \eta \frac{\partial v_z}{\partial \eta} + v_z = \frac{1}{\bar{\beta}_\theta \bar{\nu}(\eta)} \left(\frac{3}{2} \frac{\partial b_r}{\partial \eta} - \sqrt{\frac{\bar{\beta}_\theta}{\bar{\beta}_z}} \frac{\partial^2 v_\theta}{\partial \eta^2}\right) + \left(1 + \frac{1}{\bar{\beta}_\theta \bar{\nu}(\eta)}\right) \frac{\partial^2 v_r}{\partial \eta \partial \rho} + L_z v_r, \quad (98)$$

where  $L_z$  is the linear ordinary differential operator:

$$L_z v_r = \bar{D}_N \frac{\partial v_r}{\partial \eta} - \bar{D}_\Omega \left[ \left(1 + \frac{1}{\bar{\beta}_\theta \bar{\nu}(\eta)}\right) \frac{\partial}{\partial \eta} \left( \eta \frac{\partial v_r}{\partial \eta} \right) - \frac{\partial(\eta^2 v_r)}{\partial \eta} \right] + \bar{D}_B \frac{1}{\bar{\beta}_\theta \bar{\nu}(\eta)} \frac{\partial v_r}{\partial \eta}. \quad (99)$$

Note that in the important particular case of pure hydrodynamic discs the equilibrium and perturbed components of the magnetic field should be set to zero, i.e.  $\bar{\beta}_\theta = \bar{\beta}_z = \infty$  and  $b_r = b_\theta = 0$ , then Eqs. (96) - (97) with the properly resolved uncertainty in  $\bar{\beta}_\theta / \bar{\beta}_z$  are satisfied identically, and Eq. (98) is replaced by

$$\frac{1}{\Omega^2} \frac{\partial^2 v_z}{\partial t^2} - \frac{\partial^2 v_z}{\partial \eta^2} + \eta \frac{\partial v_z}{\partial \eta} + v_z = \frac{\partial^2 v_r}{\partial \eta \partial \rho} + \bar{D}_N \frac{\partial v_r}{\partial \eta} - \bar{D}_\Omega \left[ \frac{\partial}{\partial \eta} \left( \eta \frac{\partial v_r}{\partial \eta} \right) - \frac{\partial(\eta^2 v_r)}{\partial \eta} \right]. \quad (100)$$

The above problems formulated for the magnetized and magnetic-field free discs are complemented by the boundary condition of least possible divergence at infinity for the axial velocity, and in the case of magnetized discs the vanishing conditions for the in-plane magnetic-field components should be also satisfied.

An important result is immediately seen from the above set of linearized equations: to leading order in  $\epsilon$ : Eqs. (91)-(92) decouple from the rest of the system in the thin disc approximation. Note additionally that Eq. (95) for the radial magnetic field, explicitly determined by the radial velocity, may be solved separately from the rest Alfvén-mode sub-system. Thus, the sub-system (91)-(92) describes pure hydrodynamic in-plane inertia-Coriolis waves, and signifies the decoupling of the latter from the Alfvén waves. This occurs due to the negligibly small values of the projections on the disc plane of the pressure gradient and Lorentz force in the momentum balance equations (of the order of  $\epsilon^2$ ) compared with the inertial terms (of the order of  $\epsilon^0$ ) in the thin disc approximation. Thus, in the case of poloidal-dominated equilibrium, the magnetic field is of order  $\epsilon^0$  which renders the Lorentz force of the same order of magnitude as the inertial terms, and thus couples the Lorentz and inertia forces. This results in the coupling of the coriolis and Alfvén waves that eventually leads to the MRI. In contrast, the case of the toroidal-dominated magnetic field inevitably results in the scaling  $\bar{B}_z \sim \epsilon$ . This, as indicated above, means that the radial and azimuthal components of the Lorentz force are negligible with respect to the corresponding components of the inertial forces in the radial and azimuthal components of the momentum equation. As is already apparent, that decoupling between the inertial and Lorentz forces causes to a crucial deviation from the former case (i.e., with poloidal-dominated equilibrium magnetic field) and leads to the removal of the mechanism that is responsible to the MRI.

### 4.3 Linear stability problem.

The perturbations may be presented as follows

$$f(\rho, \eta, t) = \exp[-i\lambda \bar{\Omega}(\rho)t] \hat{f}(\rho, \eta), \quad (101)$$

where  $\lambda = \omega / \bar{\Omega}$  is the scaled frequency.

*Inertia-Coriolis modes.* Substituting (101) into (91) - (92) yields:

$$-i\lambda \hat{v}_r - 2\hat{v}_\theta = 0, \quad (102)$$

$$-i\lambda \hat{v}_\theta + \frac{1}{2} \hat{v}_r = 0. \quad (103)$$

The corresponding dispersion relation is therefore given by

$$\lambda = \pm 1, \quad (104)$$

which represents, the stable epicyclic oscillations in the disc plane, since for Keplerian rotation, the epicyclic frequency equals to Keplerian one,  $\bar{\chi}(\rho) = \bar{\Omega}(\rho)$ . As  $\rho$  and  $\eta$  are mere parameters each ring  $\rho = \text{const}$ ,  $\eta = \text{const}$  vibrates independently in its own plane. If viscous stresses are taken into account, an axial profile is imposed due to the mutual shear stresses between the rings and each entire cylindrical shell vibrates independently. This is indeed the case that has been solved in [Umurhan et al. (2006); Rebusco et al. (2009)]; Shtemler et al. (2010)]. As the axial and radial coordinates play the role of passive parameters, the eigenfunctions of the inertia-Coriolis modes are determined up to arbitrary amplitude  $A(\rho, \eta)$  from (102)-(104):

$$\hat{v}_\theta = \mp i \frac{1}{2} \hat{v}_r = \mp i \frac{1}{2} A(\rho, \eta). \quad (105)$$

Since any special form of the function represents some given set of initial conditions, the following self-similar separable form of the planar velocities is considered as an example:

$$A(\rho, \eta) = F(\rho)G(\eta), \quad (106)$$

where the  $F(\rho)$  and  $G(\eta)$  are arbitrary functions.

*Magnetosonic modes.* For frequencies that are different from the eigenvalues of inertial waves, namely  $\lambda \equiv \omega/\Omega(\rho) = \pm 1$  in (104), both the perturbed in-plane components of the velocity as well as the radial component of the perturbed magnetic field are zero, i.e.  $\hat{v}_r = \hat{v}_\theta = \hat{b}_r \equiv 0$ . Therefore, the perturbed axial velocity, number density, as well as the toroidal magnetic field are described by the set of equations that governs the dynamics of the magnetosonic waves:

$$\left[1 + \frac{1}{\bar{\beta}_\theta \bar{\nu}(\eta)}\right] \frac{d^2 \hat{v}_z}{d\eta^2} - \eta \frac{d\hat{v}_z}{d\eta} + (\lambda^2 - 1)\hat{v}_z = 0, \quad (107)$$

$$-i\lambda \frac{\hat{v}}{\bar{\nu}(\eta)} + \frac{d\hat{v}_z}{d\eta} - \eta \hat{v}_z = 0, \quad (108)$$

$$-i\lambda \hat{b}_\theta + \frac{d\hat{v}_z}{d\eta} = 0, \quad (109)$$

is subject to the boundary conditions at infinity of the least possible divergence for the axial velocity and the vanishing conditions for the in-plane magnetic-field components. Partial solutions are presented below .

(i) *The pure hydrodynamic system.* First start with a simple exact solution for the pure hydrodynamic system. Accounting to Eq. (100) this yields

$$\frac{d^2 \hat{v}_z}{d\eta^2} - \eta \frac{d\hat{v}_z}{d\eta} + (\lambda^2 - 1)\hat{v}_z = 0, \quad (110)$$

$$-i\lambda \frac{\hat{v}}{\bar{\nu}(\rho)} + \frac{d\hat{v}_z}{d\eta} - \eta \hat{v}_z = 0, \quad (111)$$

complemented by the boundary condition of least possible divergence at infinity for the axial velocity. That problem is degenerated to the sound waves, and coincides with the case of the poloidal-dominated equilibrium magnetic field, and its solution is:

$$\lambda = \pm \Lambda_S = \pm \sqrt{m+1}, \quad \hat{v}_z = -i\lambda W(\rho)H_m(\eta), \quad \frac{\hat{v}}{\bar{\nu}} = W(\rho)H_{m+1}(\eta) \quad \text{at } \eta = \pm\infty. \quad (112)$$

Here  $\lambda$  are the radius-independent eigenvalues;  $W(\rho)$  are the radius-dependent amplitude factors;  $H_m(\eta)$ ,  $m = 0, 1, 2, \dots$  are the Hermite polynomials.

(ii) *The limit of large plasma beta in magnetized discs.* The WKB approximation is employed now. In general, it may be applied for a wide range of plasma beta values. However, in order to simplify calculations, we restrict ourselves here by its application to the limit of large but finite values of the plasma beta. Such approach is necessary as a simple asymptotic expansion in large plasma beta  $\bar{\beta}_\theta$  fails at large  $\eta$  (small  $\bar{\nu}(\eta)$ ) due to the non-uniform limit of  $\bar{\beta}_\theta \bar{\nu}(\eta)$  in Eq. (107). As a first step the following equation for  $\hat{b}_\theta$  is derived from the system (107) - (109)

$$\frac{d^2 \hat{b}_\theta}{d\eta^2} - \eta \frac{\bar{\beta}_\theta^2 \bar{\nu}(\eta) - 1}{\bar{\beta}_\theta^2 \bar{\nu}(\eta) + \bar{\beta}_\theta} \frac{d\hat{b}_\theta}{d\eta} + (\lambda^2 - 1) \frac{\bar{\beta}_\theta \bar{\nu}(\eta)}{1 + \bar{\beta}_\theta \bar{\nu}(\eta)} \hat{b}_\theta = 0, \quad (113)$$

with the following boundary conditions:

$$\hat{b}_\theta = 0 \quad \text{at } \eta = \pm\infty. \quad (114)$$

To reduce Eq. (113) to the form appropriate for WKB approximation, the dependent variable is transformed in the following way in order to eliminate terms with first order derivatives:

$$\hat{b}_\theta = Q \int \mu d\eta, \quad \mu = \frac{\eta}{2\bar{\beta}_\theta} \frac{\bar{\beta}_\theta^2 \bar{\nu}(\eta) - 1}{\bar{\beta}_\theta \bar{\nu}(\eta) + 1}. \quad (115)$$

Then

$$\frac{d^2 Q}{d\eta^2} + \varkappa^2(\eta)Q = 0, \quad (116)$$

where

$$\varkappa^2(\eta) = -\eta^2 \frac{1 + \bar{\beta}_\theta}{2\bar{\beta}_\theta} \frac{\bar{\beta}_\theta \bar{\nu}(\eta)}{[1 + \bar{\beta}_\theta \bar{\nu}(\eta)]^2} - \frac{1}{2\bar{\beta}_\theta} \frac{1 - \bar{\beta}_\theta^2 \bar{\nu}(\eta)}{1 + \bar{\beta}_\theta \bar{\nu}(\eta)} - \eta^2 \frac{1}{4\bar{\beta}_\theta^2} \left[ \frac{1 - \bar{\beta}_\theta^2 \bar{\nu}(\eta)}{1 + \bar{\beta}_\theta \bar{\nu}(\eta)} \right]^2 + (\lambda^2 - 1) \frac{\bar{\beta}_\theta \bar{\nu}(\eta)}{1 + \bar{\beta}_\theta \bar{\nu}(\eta)}. \quad (117)$$

The approximate solutions appropriate to real and imagine  $\varkappa(\eta)$ , at which the solution oscillates and decrease, respectively, are as follows (see e.g. Migdal (1977)):

$$Q = \frac{W}{\sqrt{\varkappa(\eta)}} \exp(\pm i \int \varkappa(\eta) d\eta) \quad \text{and} \quad \bar{Q} = \frac{W}{\sqrt{|\varkappa(\eta)|}} \exp(\pm \int |\varkappa(\eta)| d\eta). \quad (118)$$

The regions of each of the solutions given in Eq. (118) are determined by the turning points which are the zeros of  $\varkappa(\eta)$ . It can be easily seen that large-plasma beta approximation is uniformly valid in the region between the turning points, and violated at large  $\eta$  due to uncertainty in the term  $\bar{\beta}_\theta \bar{\nu}(\eta)$  in (117) for exponentially vanishing  $\bar{\nu}(\eta) = \exp(-\eta^2/2)$  at  $\eta \rightarrow \pm\infty$  and  $\bar{\beta}_\theta \sim \beta \gg 1$ . Since application of the WKB method is justified asymptotically at large frequency  $\lambda$ , Eq. (117) is considered for large but fixed values of  $\bar{\beta}_\theta$  and  $\lambda$ , and for such large  $\eta$  that both  $\bar{\beta}_\theta \bar{\nu}(\eta)$  and  $\bar{\beta}_\theta^2 \bar{\nu}(\eta)$  are small. Then Eq. (117) yields to leading order

$$\varkappa^2(\eta) \approx -\frac{1}{2\bar{\beta}_\theta} \left(1 + \frac{\eta^2}{2\bar{\beta}_\theta}\right), \quad \mu(\eta) \approx -\frac{1}{2\bar{\beta}_\theta} \eta. \quad (119)$$

Choosing the minus sign to satisfy the boundary condition (114) in the approximate solution (118) for  $|\eta| > |\eta_*|$ , yields the following form for sufficiently large  $\eta$ :

$$\hat{b}_\theta \sim \frac{1}{|\varkappa|} \exp\left(-\frac{\eta^2}{4\bar{\beta}_\theta} \pm \int_{\eta_*}^{\eta} |\varkappa| d\eta\right) = \frac{2\bar{\beta}_\theta}{\eta^2} \exp\left(-\frac{\eta^2}{2\bar{\beta}_\theta}\right). \quad (120)$$

To further simplify the calculations, assume additionally that  $\bar{\beta}_\theta \gg 1$ , then the large beta limit is uniformly valid within the interval  $|\eta| \leq |\eta_*|$ , and  $\varkappa$  and  $\mu$  are given by

$$\varkappa^2(\eta) \approx -\frac{1}{4}(\eta^2 - \eta_*^2), \quad \mu(\eta) \approx \frac{1}{2}\eta, \quad (121)$$

where  $\eta_* = \pm\sqrt{4\lambda^2 - 2}$  are the turning points of the equation (116) which separate the regions of oscillatory and exponentially decreasing behavior of the solution. Thus,  $\varkappa = 0$  at  $|\eta| = |\eta_*|$ ,  $\varkappa^2$  is positive within the inner region  $|\eta| \leq |\eta_*|$  and negative otherwise within the outer region. To completely determine the problem solution, the conventional WKB approximation applies the matching conditions to the solutions (118) in the inner ( $|\eta| \leq |\eta_*|$ ) and outer ( $|\eta| \geq |\eta_*|$ ) regions in order to obtain the coefficients in (118) and the eigenvalue equation. The result is the following Bohr-Zommerfeld condition [Landau & Lifshits (1997)] that determines the dispersion relation

$$\int_{-\eta_*}^{+\eta_*} \varkappa d\eta = \pi\left(m + \frac{1}{2}\right), \quad (122)$$

where  $\varkappa$  is given by (121), and  $m$  is the number of zeros of the solution within the inner region. Substituting (121) into (122) yields

$$\lambda = \pm\sqrt{m+1}. \quad (123)$$

The eigenvalues (123) exactly coincide with those in (112) obtained with no restrictions on the value of axial wave numbers  $m$  for the pure hydrodynamic system.

Finally note that although the WKB method is valid asymptotically for large frequencies,  $\lambda \gg 1$  (i.e. large axial wave numbers,  $m$ ), it frequently yields a fair approximation up to finite values  $\lambda \sim 1$  [see e.g. Migdal (1977)]. This allows expecting that eigenvalues (123) will be appropriate even for low axial wave numbers  $m = 1, 2, \dots$

(iii) *The limit of small plasma beta in magnetized discs.* Consider the problem (107) -(109) in the limit of small plasma beta  $\bar{\beta}_\theta(\rho) \sim \bar{\beta} \ll 1$ . Assuming simultaneously that the eigenvalue  $\lambda$  is large, so that  $\lambda^2 \bar{\beta}_\theta \sim \bar{\beta}^0$ , Eq. (107) yields to leading order in small  $\bar{\beta}$

$$\frac{d^2 \hat{v}_z}{d\eta^2} + \lambda^2 \bar{\beta}_\theta \bar{\nu}(\eta) \hat{v}_z = 0. \quad (124)$$

Replacing as in Section 3.3 the steady-state isothermal density distribution  $\bar{\nu}(\eta) = \exp(-\eta^2/2)$  by the hyperbolic function  $\bar{\nu}(\eta) = \text{sech}^2(b\eta)$  with  $b = \sqrt{2/\pi}$ , and introducing the auxiliary variable  $\xi = \tanh(b\eta)$ , transform Eq. (124) to the following form:

$$L\hat{v}_z + \bar{\lambda}^2 \hat{v}_z = 0, \quad (125)$$

where  $L$  is the Legendre differential operator of second order,

$$L \equiv \frac{d}{d\xi} \left[ (1-\xi^2) \frac{d}{d\xi} \right],$$

and  $\bar{\lambda}^2$  is given by:

$$\bar{\lambda}^2 = \frac{1}{b^2} \lambda^2(\rho) \bar{\beta}_\theta(\rho) \sim \bar{\beta}^0. \quad (126)$$

Imposing now that  $\hat{v}_z$  diverges polynomially at most when  $\eta \rightarrow \infty$ , leads to the conclusion that the solution of Eq. (126) for  $\hat{v}_z$  is proportional to the Legendre polynomials  $P_m(\xi)$ :



$$\frac{\hat{v}_z}{W(\rho)} = P_m(\xi) \sim \bar{\beta}^0, \quad \bar{\lambda}^2 = m(m+1) \sim \bar{\beta}^0, \quad m = 1, 2, \dots \quad (127)$$

Equations (105) - (106) yield that  $\hat{b}_\theta$  and  $\hat{v}$  are of higher order in small plasma beta:

$$\begin{aligned} \frac{\hat{b}_\theta}{W(\rho)} &= -i \sqrt{\frac{m}{m+1}} [P_{m-1}(\xi) - \xi P_m(\xi)] \bar{\beta}_\theta^{1/2} \sim \bar{\beta}^{1/2}, \\ \frac{\hat{v}}{W(\rho)} &= \frac{i}{b} \sqrt{\frac{m}{m+1}} (1 - \xi^2) \left[ \left( \xi + \frac{1}{mb} \operatorname{arctanh} \xi \right) P_m(\xi) - P_{m-1}(\xi) \right] \bar{\beta}_\theta^{1/2} \sim \bar{\beta}^{1/2}. \end{aligned} \quad (128)$$

Since  $P_m(1) = 1$  and  $P_m(-1) = (-1)^m$  for all  $m$ ,  $\hat{b}_\theta$  satisfies the vanishing boundary condition at infinity  $\eta \rightarrow \pm\infty$  ( $\xi \rightarrow \pm 1$ ).

Thus, summarizing, the main conclusion from both limits (high and low plasma beta) is that the inertia-Coriolis waves are decoupled from the Alfvén waves, which henceforth leads to the complete stabilization of the MRI's. This, as will be subsequently seen, leaves the stage exclusively to the non modal algebraic growth mechanism. Remarkably that both limits assume sufficiently large values of the eigenvalues (scaled frequencies  $\lambda$ ): in the limit of large  $\beta$  in (123) due to high frequency assumption inherent to WKB, while in opposite limit of small  $\beta$  in (127), because to asymptotic behavior of  $\lambda \sim \beta^{-1/2}$ .

#### 4.4 Non-resonantly and resonantly driven magnetosonic modes

There are two mechanisms responsible for algebraic time-growth of perturbations, namely non-resonant and resonant excitation of vertical magnetosonic waves by planar inertia-Coriolis modes. This fact for the pure hydrodynamic adiabatic discs was established in [Umurhan et al. (2006); Rebusco et al. (2009)]; Shtemler et al. (2010)]. As shown below, both mechanisms are also relevant in a modified form for vertically-isothermal magnetized discs. Due to the rotation shear effect and the presence of radial derivatives in the system (94) -(100), the amplitude of the magnetosonic modes driven by the inertia-Coriolis modes grows linearly in time in the case when the magnetosonic mode frequency is not equals to the inertial-Coriolis one. While for the same frequencies of the magnetosonic and inertial-Coriolis modes, the latter grows quadratically in time.

To demonstrate linear and quadratic in time growth of the perturbations, both non-resonantly and resonantly driven modes are illustrated below by simple explicit solutions. The non-resonantly driven magnetosonic waves are considered in the limit of small toroidal plasma beta and for pure hydrodynamic system, as typical examples. Noting that the resonantly driven magnetosonic modes may exist for arbitrary frequencies, we restrict ourselves by considering a pure hydrodynamic system which is characterized by simple explicit solutions with no limitation on the frequency value.

The driving modes are characterized by Eqs. (101) and (105). As a result, the driven magnetosonic or sound modes in magnetized or magnetic-field free discs, i.e. (98) or (100), respectively, are described by the following expressions:

$$\{v_r, v_\theta, b_\theta\} = \exp[-i\lambda\bar{\Omega}(\rho)t] \{\hat{v}_r, \hat{v}_\theta, \hat{b}_\theta\}(\rho, \eta, t). \quad (129)$$

Inserting then Eq. (129) into the system of equations ((93)-(100) and keeping only terms that are proportional to  $t$  on their right hand sides yields

$$\frac{1}{\bar{\Omega}^2} \frac{\partial^2 v_z}{\partial t^2} - \left(1 + \frac{1}{\bar{\beta}_\theta \bar{\nu}(\eta)}\right) \frac{\partial^2 v_z}{\partial \eta^2} + \eta \frac{\partial v_z}{\partial \eta} + v_z = \mp i t \exp[-i\lambda\bar{\Omega}(\rho)t] \left(1 + \frac{1}{\bar{\beta}_\theta \bar{\nu}(\eta)}\right) \frac{d\bar{\Omega}}{d\rho} \frac{\partial \hat{v}_r}{\partial \eta}, \quad (130)$$

$$\frac{1}{\bar{\Omega}} \frac{\partial}{\partial t} \left[ \frac{\nu}{\bar{\nu}(\eta)} \right] + \frac{\partial v_z}{\partial \eta} - \eta v_z = \pm i t \exp[\mp i\bar{\Omega}(\rho)t] \frac{d\bar{\Omega}}{d\rho} \hat{v}_r, \quad (131)$$

$$\frac{1}{\bar{\Omega}} \frac{\partial b_\theta}{\partial t} + \frac{\partial v_z}{\partial \eta} = \pm i t \exp[\mp i\bar{\Omega}(\rho)t] \frac{d\bar{\Omega}}{d\rho} \hat{v}_r. \quad (132)$$

The problems (130)-(132) is subject to the boundary condition of least possible divergence for the axial velocity, and for the magnetized discs complemented by the vanishing conditions of the toroidal magnetic field at  $\eta = \pm\infty$ . As is indeed seen from that system, the magnetosonic wave is driven by the inertial wave, while the linear growth in time is entirely due to effect of the rotation shear, and disappears for  $d\bar{\Omega}/d\rho = 0$ .

As was mentioned above the two limits of small toroidal plasma beta as well as pure hydrodynamic system are considered analytically. If the scaled eigen-frequency of the inertia-coriolis waves (108),  $\lambda = \pm 1$ , do not coincide with the eigen-frequencies of the magnetosonic waves (117),  $\lambda = \pm\sqrt{m+1}$ , i.e. at  $m \neq 0$ , non-resonantly driven magnetosonic modes are excited. The stable magnetosonic modes may be excited resonantly by the inertial modes if any pair of respective eigen-values (108) with  $\lambda = \pm 1$  and (117) with  $\lambda = \pm\sqrt{m+1}$ , coincide. It is easy to see that this may happen only for  $m = 0$ .

(i) *Non-resonantly driven magnetosonic modes in the limit of small plasma beta.* At vanishing plasma beta,  $\beta$ , in the leading order approximation Eq. (130) leads to a degenerate quasi-steady problem for  $\hat{v}_z$  on the Keplerian time scale. Twice integrating Eq. (130) in  $\eta$  and setting arbitrary integration constants to zero, yield:

$$\hat{v}_z = \pm i \frac{d\bar{\Omega}}{d\rho} \int_0^\eta \hat{v}_r d\eta. \quad (133)$$

The rest unknown number density and toroidal magnetic field can be found at known  $\hat{v}_z$  from non-degenerate unsteady relations (131) -(132).

(ii) *Non-resonantly and resonantly driven magnetosonic modes in pure hydrodynamic discs.* Setting  $\bar{\beta}_\theta \equiv \infty$ ,  $\hat{v}_r$  on the right-hand sides of (130) -(132) may be expanded in terms of the complete set of the spatial eigen-functions for the magnetosonic mode, namely, in the Hermite polynomials:

$$\hat{v}_r(\rho, \eta) = \sum_{m=0} W_{r,m}(\rho) H_m(\eta). \quad (134)$$

Examining the effect of a single term in the expansion above and utilizing the following recursion relation for the Hermite polynomials:

$$\frac{dH_m}{d\eta} = mH_{m-1}(\eta), \quad m = 1, 2, \dots,$$

substituting the exponential ansatz (129) into Eq. (100), and keeping only terms that are proportional to  $t$  on its right hand side yield

$$\frac{1}{\Omega^2} \frac{\partial^2 v_{z,m-1}}{\partial t^2} - \frac{\partial^2 v_{z,m-1}}{\partial \eta^2} + \eta \frac{\partial v_{z,m-1}}{\partial \eta} + v_{z,m-1} = \mp i t \exp[\mp i \bar{\Omega}(\rho) t] \frac{d\bar{\Omega}}{d\rho} W_{r,m-1}(\rho) m H_{m-1}(\eta), \quad (135)$$

where for  $m = 1$  the right hand side of Eq. (135) is a solution of the homogeneous part of the equation and hence represents a resonant driving force. For any other value of  $m$  the magnetosonic waves are driven non-resonantly. The typical non-resonant ( $m = 2$ ) and resonant ( $m = 1$ ) solution of Eq. (135) may be written in the following form:

$$v_{z,m-1} = \hat{v}_{z,m-1}(\rho, \eta, t) \exp[\mp i \bar{\Omega}(\rho) t] = \mp i \exp[\mp i \bar{\Omega}(\rho) t] W_{z,m-1}(\rho, t) H_{m-1}(\eta), \quad (136)$$

$$W_{z,1}(\rho, t) = (it\bar{\Omega})W_{z,1}^{(1)}(\rho) + W_{z,1}^{(0)}(\rho) \quad \text{for } m = 2, \quad (137)$$

$$W_{z,0}(\rho, t) = \frac{(it\bar{\Omega})^2}{2} W_{z,0}^{(2)}(\rho) + (it\bar{\Omega})W_{z,0}^{(1)}(\rho) \quad \text{for } m = 1. \quad (138)$$

Here the coefficients are determined through an arbitrary amplitude of the radial velocity  $W_{r,1}(\rho)$  for non-resonant ( $m = 2$ ) and resonant ( $m = 1$ ) system, respectively, are as follows

$$\frac{W_{z,1}^{(1)}(\rho)}{W_{r,1}(\rho)} = -i \frac{2}{\bar{\Omega}} \frac{d\bar{\Omega}}{d\rho}, \quad \frac{W_{z,1}^{(0)}(\rho)}{W_{r,1}(\rho)} = \pm i \frac{2}{\bar{\Omega}} \frac{d\bar{\Omega}}{d\rho} \quad \text{for } m = 2, \quad (139)$$

$$\frac{W_{z,0}^{(2)}(\rho)}{W_{r,1}(\rho)} = \mp i \frac{1}{\bar{\Omega}} \frac{d\bar{\Omega}}{d\rho}, \quad \frac{W_{z,0}^{(1)}(\rho)}{W_{r,1}(\rho)} = -i \frac{1}{2} \frac{1}{\bar{\Omega}} \frac{d\bar{\Omega}}{d\rho} \quad \text{for } m = 1. \quad (140)$$

The corresponding expressions for number density and toroidal magnetic field may be derived from the rest equations of the system (131) -(132).

## 5 SUMMARY AND DISCUSSION

A comprehensive asymptotic analysis in small aspect ratio of the disc,  $\epsilon$ , has been carried out of the response of thin vertically-isothermal Keplerian discs to small magnetohydrodynamic perturbations. Two regimes of axisymmetric instability have been identified depending on the type of equilibria in small aspect ratio of the disc,  $\epsilon$ . The first is developed in the axially dominated equilibrium magnetic configurations,  $\bar{B}_z \sim \epsilon^0$ , and is excited at a relatively low level of hydrodynamic perturbations in the disc plane  $V'_r, V'_\theta \sim \epsilon^1$ , while the second regime occurs in the toroidally dominated magnetic fields,  $\bar{B}_\theta \sim \epsilon^0$ , at relatively high level of hydrodynamic perturbations,  $V'_r, V'_\theta \sim \epsilon^0$  (the axial velocity perturbations are in both regimes of the same orders,  $V'_z \sim \epsilon^1$ , see Tables 1 and 2). As a result of that scaling, the pure hydrodynamic limit is achievable only within the second regime. Indeed, it is demonstrated that as distinct from the first regime, the second regime can not produce spectrally unstable modes, but excites a weak algebraic non-modal growth in time. The inertia-Coriolis driven magnetosonic mode leads to their non-resonant and resonant coupling that induces, respectively, the linear and quadratic in time growth of perturbations. It should be emphasized though that that result is restricted to axisymmetric perturbations and nonaxisymmetric ones may give rise to spectral instabilities in the dominant toroidal field case as well, as indeed is the case for magnetized Taylor-Couette flows (see Rudiger et al. 2007).

Solutions of the stability problem for I type equilibria are obtained by replacing the true isothermal density vertical steady-state distribution  $\bar{v}(\eta) = \exp(-\eta^2/2)$  by the hyperbolic function  $\bar{v}(\eta) = \text{sech}^2(b\eta)$  which has the similar shape and the same total mass of the disc. This model profile represents some true equilibrium that is obtained from a slightly different gravitational potential. The model eigenfunctions are exact solutions of the model very close to those obtained approximately by WKB from the true problem [Liverts & Mond (2009)]. They form the full family of explicit, simple and orthogonal

eigenfunctions of the model problem. Such properties are significant for the consequent study of non-linear development of the instability.

The model of the non-modal instability [Shtemler et al. (2010)] for pure hydrodynamic adiabatic discs is adopted in the present work for more realistic vertically-isothermal discs with diffused density vanishing at infinity. The model is also extended on magnetized discs with II type equilibria. Within that model the eigenvalue problem has been solved in the characteristic cases of small and large plasma beta as well as for pure hydrodynamic systems. Furthermore, the non-resonantly driven magnetosonic waves are considered in the limit of small toroidal plasma beta, as a typical example. Since in the limits of large and small plasma beta, the magnetosonic modes are excited with high scaled frequency,  $\lambda \gg 1$ , they can not be resonantly driven by the low-frequency inertial-Coriolis mode with  $\lambda \pm 1$ . By this reason the resonantly driven magnetosonic modes are calculated for only the pure hydrodynamic system, in order to illustrate a quadratic in time growth of perturbations. The rotation shear is found to be responsible for the linear and quadratic growth in time. Furthermore, compressible inertia-coriolis stable oscillations continuously pump energy from the sheared steady state equilibrium and transfer it (resonantly as well as non resonantly) to the continuously algebraically growing magnetosonic waves. Compressibility is indeed inevitable due to the supersonic rotation of the steady-state disc combined with its small vertical dimensions which make the vertical magnetosonic crossing time of the order of a rotation period. As distinct from MRI the non modal growth is exhibited for all admissible parameters of the system.

## REFERENCES

- Balbus S. A., & Hawley J. F., 1991, ApJ, **376**, 214  
 Begelman M.C. & Pringle J.E., 2007, MNRAS, **375**, 1070  
 Bodo G., Mignone A., Cattaneo F., Rossi P., and Ferrari A., A&A, **487**, 1  
 Chandrasechar S., 1960, Proc. Natl. Acad. Sci. A, **46**, 46, 223  
 Coppi B., & Keyes E.A., 2003, ApJ, **595**, 1000  
 Frank J., King A., and Raine D., 2002, *Acreation Power in Astrophysics* , (Cambridge: University Press).  
 Fromang S., and Papaloizou J., 2007, A&A, **476**, 1113  
 Fromang S., Papaloizou J., Lesur G., Heineman T., 2007, A&A, **476**, 1123  
 Hawley J. F., & Krolik J. H., 2002, ApJ, **566**, 164  
 Landau L. D. and Lifshits E. M., 1977, *Quantum mechanics, Non-Relativistic Theory* , (Pergamon Press).  
 Lesur G., and Longaretti P. Y., 2007, MNRAS, **378**, 1471  
 Liverts E. and Mond M., 2009, MNRAS, **392**, 287  
 Migdal A. B., 1977, *Qualitative Methods in Quantum Physics*, (Massachusetts: W. A. Bnejamin Inc.).  
 Papaloizou J. C. B., & Terquem C., 1997, MNRAS, **287**, 771  
 Pessah M.E. and Psaltis D., 2005, ApJ, **628**, 829  
 Pessah M. E., Chan C. K., Psaltis D., 2007, ApJ, **668**, L51  
 Proga D., 2003, ApJ, **585** 406  
 Rebusco P., Umurhan O. M., Kluzniak W., and Regev O., 2009, Phys. Fluids, **21**, 076601  
 Regev O., and Umurhan O. M., 2008, A&A, **481**, 21  
 Rudiger G., Hollerbach R., Schultz M., and Detlev E., 2007, MNRAS, **377**, 1481  
 Shtemler Y. M., Mond M., & Rudiger G., 2009, MNRAS, **394**, 1379  
 Shtemler Y. M., Mond M., Rudiger G, Regev O., & Umurhan O.M., 2010, MNRAS, **406**, 517  
 Spitzer L., 1942, The Astronomical Journal, **95**, 329  
 Terquem C., & Papaloizou J. C. B., 1996, MNRAS, **279**, 767  
 Velichov E. P., 1959, Zh. Eksp. Teor. Fiz., **36**, 1398 [English translation, 1959, Sov. Phys. JETP, 36, 95]  
 Umurhan O. M., Nemirovsky A., Regev O., & Shaviv G., 2006, A&A, **446**, 1